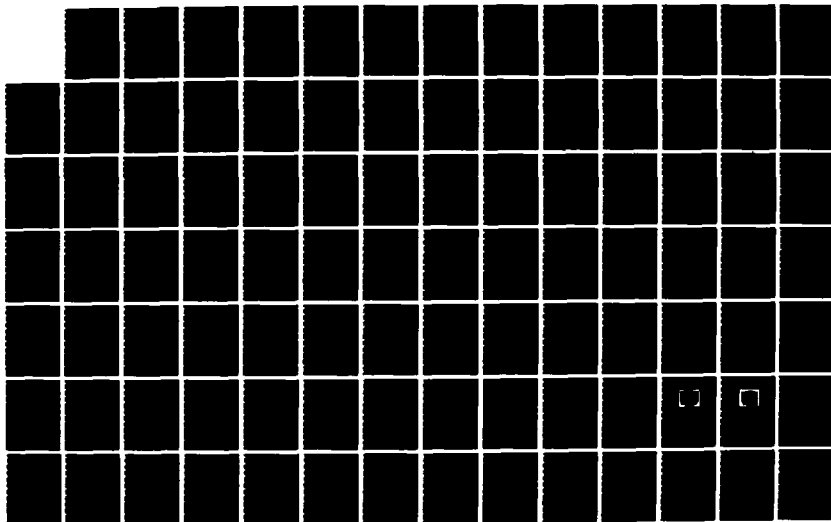LOW NOISE AMPLIFIER FOR USE WITH SUBMILLIMETER
ELECTRIC-FIELD PROBES(U) ARMY MILITARY PERSONNEL CENTER
ALEXANDRIA VA  S PAVLICA MAY 87

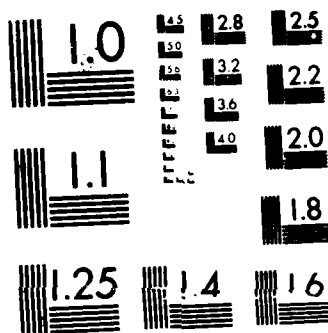MICROCOPY RESOLUTION TEST CHART

NATIONAL BUREAU OF STANDARDS-1963 A

AD-A180 132

Low Noise Amplifier for Use with Submillimeter Electric-Field Probes

CPT Steve Pavlica
HQDA, MILPERCEN (DAPC-OPA-E)
200 Stovall Street
Alexandria, VA.    22332

Final Report   May 1987

A thesis submitted to the Faculty of the School of Engineering and
Applied Science, University of Virginia, in partial fulfillment
of the requirements for the degree  of Master of Science Electrical
Engineering.

87-5-11-022

| REPORT DOCUMENTATION PAGE | | READ INSTRUCTIONS BEFORE COMPLETING FORM |
|---|---|---|
| 1. REPORT NUMBER | 2. GOVT ACCESSION NO. | 3. RECIPIENT'S CATALOG NUMBER |
| 4. TITLE (and Subtitle) <br><br> Low Noise Amplifier for Use with Electric Field Probes | | 5. TYPE OF REPORT & PERIOD COVERED <br><br> Final Report  May 1987 |
| | | 6. PERFORMING ORG. REPORT NUMBER |
| 7. AUTHOR(s) <br><br> Steve Pavlica | | 8. CONTRACT OR GRANT NUMBER(s) |
| 9. PERFORMING ORGANIZATION NAME AND ADDRESS <br> HQDA, MILPERCEN (DAPC-OPA-E) <br> 200 Stovall Street <br> Alexandria, VA.   22332 | | 10. PROGRAM ELEMENT, PROJECT, TASK AREA & WORK UNIT NUMBERS |
| 11. CONTROLLING OFFICE NAME AND ADDRESS <br> HQDA, <br> MILPERCEN, ATTN: DAPC-OPA-E <br> 200 Stovall Street, Alexandria, VA.   22332 | | 12. REPORT DATE <br> May 1987 |
| | | 13. NUMBER OF PAGES <br> 80 |
| 14. MONITORING AGENCY NAME & ADDRESS(if different from Controlling Office) | | 15. SECURITY CLASS. (of this report) <br><br> Unclassified |
| | | 15a. DECLASSIFICATION/DOWNGRADING SCHEDULE |

16. DISTRIBUTION STATEMENT (of this Report)

Approved for public release; distribution unlimited.

17. DISTRIBUTION STATEMENT (of the abstract entered in Block 20, if different from Report)

18. SUPPLEMENTARY NOTES

Thesis
Master of Science Electrical Engineering
School of Engineering and Applied Science
University of Virginia

19. KEY WORDS (Continue on reverse side if necessary and identify by block number)

E-field probe
Low noise amplifier,
Noise analysis

20. ABSTRACT (Continue on reverse side if necessary and identify by block number)

In the past several years, there has been increasing concern over the effects on human beings of low level electromagnetic radiation. Submillimeter Electric-Field probes were developed to directly measure E-fields in biological media. These probes are also very useful for measuring E-fields in cavities where solving the mathematical equations, because of the geometries of the cavities, is very difficult or impossible. An amplification system for these probes is investigated. This system is designed, built, and laboratory tested. A theoretical gain equation is developed relating

DD FORM 1473 EDITION OF 1 NOV 65 IS OBSOLETE
1 JAN 73

87    5  11  022

20 cont.

the output voltage of the system to the impinging E-field on the probe. Additionally, a complete noise analysis is accomplished. Theoretical noise work is verified in the laboratory, along with the gain equation. Finally, modulation of the probe-amplifier system is shown to be feasible and is demonstrated in the laboratory. This will allow the measurement the relative phase shift between two points in a cavity.

# INSTRUCTIONS FOR PREPARATION OF REPORT DOCUMENTATION PAGE

<u>RESPONSIBILITY</u>. The controlling DoD office will be responsible for completion of the Report Documentation Page, DD Form 1473, in all technical reports prepared by or for DoD organizations.

<u>CLASSIFICATION</u>. Since this Report Documentation Page, DD Form 1473, is used in preparing announcements, bibliographies, and data banks, it should be unclassified if possible. If a classification is required, identify the classified items on the page by the appropriate symbol.

## COMPLETION GUIDE

General. Make Blocks 1, 4, 5, 6, 7, 11, 13, 15, and 16 agree with the corresponding information on the report cover. Leave Blocks 2 and 3 blank.

<u>Block 1</u>. Report Number. Enter the unique alphanumeric report number shown on the cover.

<u>Block 2</u>. Government Accession No. Leave Blank. This space is for use by the Defense Documentation Center.

<u>Block 3</u>. Recipient's Catalog Number. Leave blank. This space is for the use of the report recipient to assist in future retrieval of the document.

<u>Block 4</u>. Title and Subtitle. Enter the title in all capital letters exactly as it appears on the publication. Titles should be unclassified whenever possible. Write out the English equivalent for Greek letters and mathematical symbols in the title *(see "Abstracting Scientific and Technical Reports of Defense-sponsored RDT/E,"AD-667 000)*. If the report has a subtitle, this subtitle should follow the main title, be separated by a comma or semicolon if appropriate, and be initially capitalized. If a publication has a title in a foreign language, translate the title into English and follow the English translation with the title in the original language. Make every effort to simplify the title before publication.

<u>Block 5</u>. Type of Report and Period Covered. Indicate here whether report is interim, final, etc., and, if applicable, inclusive dates of period covered, such as the life of a contract covered in a final contractor report.

<u>Block 6</u>. Performing Organization Report Number. Only numbers other than the official report number shown in Block 1, such as series numbers for in-house reports or a contractor/grantee number assigned by him, will be placed in thi · space. If no such numbers are used, leave this space blank.

<u>Block 7</u>. Author(s). Include corresponding information from the report cover. Give the name(s) of the author(s) in conventional order *(for example, John R. Doe or, if author prefers, J. Robert Doe)*. In addition, list the affiliation of an author if it differs from that of the performing organization.

<u>Block 8</u>. Contract or Grant Number(s) For a contractor or grantee report, enter the complete contract or grant number(s) under which the work reported was accomplished. Leave blank in in-house reports.

<u>Block 9</u>. Performing Organization Name and Address. For in-house reports enter the name and address, including office symbol, of the performing activity. *For contractor or grantee reports enter the name and address of the contractor or grantee who prepared the* report and identify the appropriate corporate division, school, laboratory, etc., of the author. List city, state, and ZIP Code.

<u>Block 10</u>. Program Element, Project, Task Area, and Work Unit Numbers. Enter here the number code from the applicable Department of Defense form, such as the DD Form 1498, "Research and Technology Work Unit Summary" or the DD Form 1634. "Research and Development Planning Summary," which identifies the program element, project, task area, and work unit or equivalent under which the work was authorized.

<u>Block 11</u>. Controlling Office Name and Address. Enter the full, official name and address, including office symbol, of the controlling office. *(Equates to funding/sponsoring agency. For definition see DoD Directive 5200.20, "Distribution Statements on Technical Documents.")*

<u>Block 12</u>. Report Date. Enter here the day, month, and year or month and year as shown on the cover.

<u>Block 13</u>. Number of Pages. Enter the total number of pages.

<u>Block 14</u>. Monitoring Agency Name and Address *(if different from Controlling Office)*. For use when the controlling or funding office does not directly administer a project, contract, or grant, but delegates the administrative responsibility to another organization.

Blocks 15 & 15a. Security Classification of the Report: Declassification/Downgrading Schedule of the Report. Enter in 15 the highest classification of the report. If appropriate, enter in 15a the declassification/downgrading schedule of the report, using the abbreviations for declassification/downgrading schedules listed in paragraph 4-207 of DoD 5200.1-R.

<u>Block 16</u>. Distribution Statement of the Report. Insert here the applicable distribution statement of the report from DoD Directive 5200.20, "Distribution Statements on Technical Documents."

<u>Block 17</u>. Distribution Statement *(of the abstract entered in Block 20, if different from the distribution statement of the report)*. Insert here the applicable distribution statement of the abstract from DoD Directive 5200.20, "Distribution Statements on Technical Documents."

<u>Block 18</u>. Supplementary Notes. Enter information not included elsewhere but useful, such as: Prepared in cooperation with . . . Translation of *(or by)* . . . Presented at conference of . . . To be published in . . .

<u>Block 19</u>. Key Words. Select terms or short phrases that identify the principal subjects covered in the report, and are sufficiently specific and precise to be used as index entries for cataloging, conforming to standard terminology. The DoD "Thesaurus of Engineering and Scientific Terms" *(TEST)*, AD-672 000, can be helpful.

<u>Block 20</u>. Abstract. The abstract should be a brief *(not to exceed 200 words)* factual summary of the most significant information contained in the report. If possible, the abstract of a classified report should be unclassified and the abstract to an unclassified report should consist of publicly- releasable information. If the report contains a significant bibliography or literature survey, mention it here. For information on preparing abstracts see *"Abstracting Scientific and Technical Reports of Defense-Sponsored RDT&E,"* AD-667 000.

# LOW NOISE AMPLIFIER FOR USE WITH
# SUBMILLIMETER ELECTRIC-FIELD PROBES

---

A Thesis

Presented to the

Faculty of the School of Engineering and Applied Science

University of Virginia

---

In Partial Fulfillment

of the requirements for the Degree

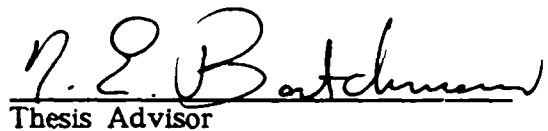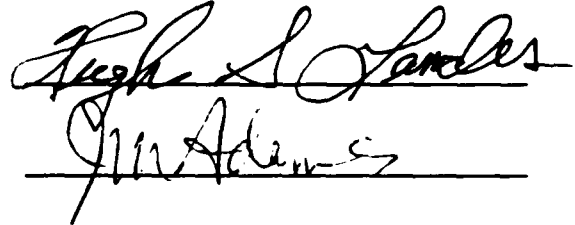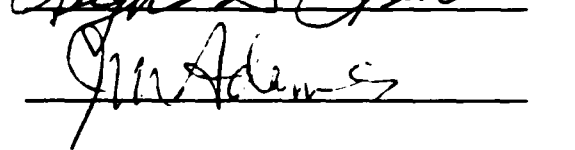Master of Science Electrical Engineering

---

by

Steve Pavlica

May 1987

# APPROVAL SHEET

This thesis is submitted in partial fulfillment of the

requirements for the degree of

Master of Science (Electrical Engineering)

_____
Author

This thesis has been read and approved by the examining Committee:

_____
Thesis Advisor

_____

_____

Accepted for the School of Engineering and Applied Science:

_____
Dean, School of Engineering
and Applied Science

May 1987

# ABSTRACT

In the past several years, there has been increasing concern over the effects on human beings of low level electromagnetic radiation. Submillimeter Electric-Field probes were developed to directly measure E-fields in biological media. These probes are also very useful for measuring E-fields in cavities where solving the mathematical equations, because of the geometries of the cavities, is very difficult or impossible. An amplification system for these probes is investigated. This system is designed, built and laboratory tested. A theoretical gain equation is developed relating the output voltage of the system to the impinging E-field on the probe. Additionally, a complete noise analysis is accomplished. Theoretical noise work is verified in the laboratory, along with the gain equation. Finally, modulation of the probe-amplifier system is shown to be feasible, and is demonstrated in the laboratory. This will allow the measurement of the relative phase shift between two points in a cavity.

i

## ACKNOWLEDGEMENTS

There are a number of people without whose invaluable support, this thesis could not have been completed.

Dr. Ted Batchman, my advisor, deserves a medal for his infinite patience. All of us in the laboratory asked him hours of questions and he found time to answer all of them, while always maintaining his perpetual smile. I owe an especially deep debt of gratitude to Dr. Hugh Landes, not only for chairing my examination committee, but most importantly, for finding the time and energy to assist me in various electrical engineering subjects when I first returned to graduate school. After being out of school for more than six years, I could not spell complex derivative, let alone solve for one.

The guys in the lab: Jim, Steve, Gene and Dave, were truly amazing. I have never seen a group of guys who were so adept at getting out of work so that they could spend time playing computer games. Guys, I still do not understand footballs in k-space, mode-locking, Q-switching, the extraordinary index of refraction, or Maxwell's equations. However, I truly appreciate your efforts.

Dr. Joe Mait is the only person I know who can go through six pages of math in less than five minutes and pinpoint why the answer came out wrong by a factor of 4.783. He was very helpful during my initial study of the mathematical properties of noise. I would also like to thank Dr. J.

Milton Adams for agreeing to serve on my examining committee, even though I did not delve into the biological aspects of E-field probes.

To all of the computer dieties: Andy, Richard, Zia, Jim, Jay and Lee, thanks for all the help.

Special thanks to James McIntosh, EE Technician, for always procuring the equipment I needed to work with, especially since some of it came from the undergraduate laboratories.

To those I have not been able to thank by name, I would like to say that your efforts have been most helpful and are most appreciated.

# TABLE OF CONTENTS

# LIST OF FIGURES

# LIST OF SYMBOLS

$C_{ant}$      dipole capacitance

$b$      dipole length

$\theta$      angle between E-field and antenna orientation

$R_b$      diode bulk resistance

$R_v$      diode video resistance

$C_j$      diode junction capacitance

$R_1$      tab resistance on lead structure

$Z_c$      transmission line impedance at source end

$R_T$      total dc resistance

$R_L$      lead resistance of transmission line

$I_j$      total current through diode's depletion region

$I_{jo}$      dc current through diode's depletion region

$V_j$      total voltage across diode's depletion region

$V_{jo}$      dc voltage across diode's depletion region

$V_{j1}$      first ac harmonic voltage across diode's depletion region

$\alpha$      reciprocal of thermal voltage

$R_x$      gain resistor in INA 110

CMRR      common mode rejection ratio

| | |
|---|---|
| $V_4$ | offset nulling voltage |
| $V_{os}$ | offset voltage |
| $R_a$ | FET gate current drive resistors |
| $\overline{i^2}$ | mean square current |
| $\overline{v^2}$ | mean square voltage |
| $\dfrac{\overline{v^2}}{\Delta f}$ | voltage power spectral density |
| $\dfrac{\overline{i^2}}{\Delta f}$ | current power spectral density |
| $\overline{v_i^2}$ | equivalent mean square input noise voltage |
| $\overline{i_i^2}$ | equivalent mean square input noise current |
| $R_s$ | source resistance |
| $\overline{v_{on}^2}$ | total output mean square noise voltage |
| $\overline{v_{R_s}^2}$ | mean square thermal noise voltage of $R_s$ |
| $\overline{i_{tin}^2}$ | total mean square noise current referred to the input of the system |
| $\overline{v_{tin}^2}$ | total mean square noise voltage referred to the input of the system |
| $\overline{i_{2R_a}^2}$ | mean square thermal noise current of $2R_a$ |
| $\overline{i_{R(\omega)}^2}$ | mean square thermal noise current of $R(\omega)$ |
| $\overline{i_{R_v}^2}$ | mean square thermal noise current of $R_v$ |
| $\Delta f$ | noise bandwidth |
| $\rho$ | correlation coefficient |

$Z_i$        input impedance of amplifier

$A_v$        amplifier gain

$K$        system gain

$S_x^z$        sensitivity of z with respect to x

$P_o$        power in waveguide

$\dfrac{P_o}{ab}$        power density in waveguide

$Z_o$        impedance of free space

LIA        lock-in amplifier

# CHAPTER 1

# INTRODUCTION

## 1.1. Introduction

In the past ten years, a considerable amount of research effort has been expended toward developing an electromagnetic field probe (E-field probe) for use in measuring low and very low intensity E-fields. H. Bassen, et al, developed a system to measure low intensity E-fields [1] using a center dipole antenna structure and a nonlinear rectifying element in the form of a diode. George Gimpelson developed an improved E-field probe in 1983 at the University of Virginia [2]. In 1986, Phil Howerton, a doctoral candidate at the University of Virginia, succeeded in miniaturization of the E-field probe. In addition, he also developed a three-axis probe, which can measure the three vector E-field components [3]. In 1984, Tom Marshburn carried Gimpelson's work further with a fairly rigorous noise and sensitivity analysis of the E-field probe, assuming a perfect amplifier (no current drawn from the probe) connected to the output of the probe [4].

The current E-field probe produces an extremely small output signal. In addition, the output impedance of the probe is very large, because of the highly resistive leads from the dipole antenna section of the probe to the output connector. These highly resistive leads are necessary to minimize the effect of the lead structure on the E-field being measured. One of the major

problems in the laboratory was the lack of amplification and signal conditioning equipment necessary to take real-time E-field measurements with the probes being built. The Bureau of Radiological Health, Department of Health and Human Services, located in Maryland, had the only equipment that could be used to test and calibrate the E-field probes, once they were manufactured here. Therefore, there exists a need to have the equipment necessary to test and calibrate the probes on an in-house basis. The purpose of this thesis is to design and analyze amplification and signal conditioning equipment that can be used with the current generation of E-field probes.

## 1.2. Discussion of E-Field Probe

This section is a review of the works in references 2, 3 and 4. It is designed to provide a working knowledge of the ac and dc characteristics of the E-field probe, so that these characteristics can be referred to in subsequent chapters.

The E-field probe consists of a short dipole antenna (600 microns), a zero-bias Schottky barrier diode (Hewlett-Packard 5082-2716 Beam Lead), and a highly resistive output transmission line. Figure 1-1 shows the general structure of the probe [3]. Figure 1-2 was extracted from [4] and is probably the most complete modeling of the high frequency characteristics of the probe. When an E-Field impinges on the dipole antenna, there is a voltage produced that is equal to Eh cos$\theta$, where $\theta$ is the angle between the E-field and the dipole antenna. The dipole also has an inherent capacitance whose magnitude is proportional to the charge separation across the leads of
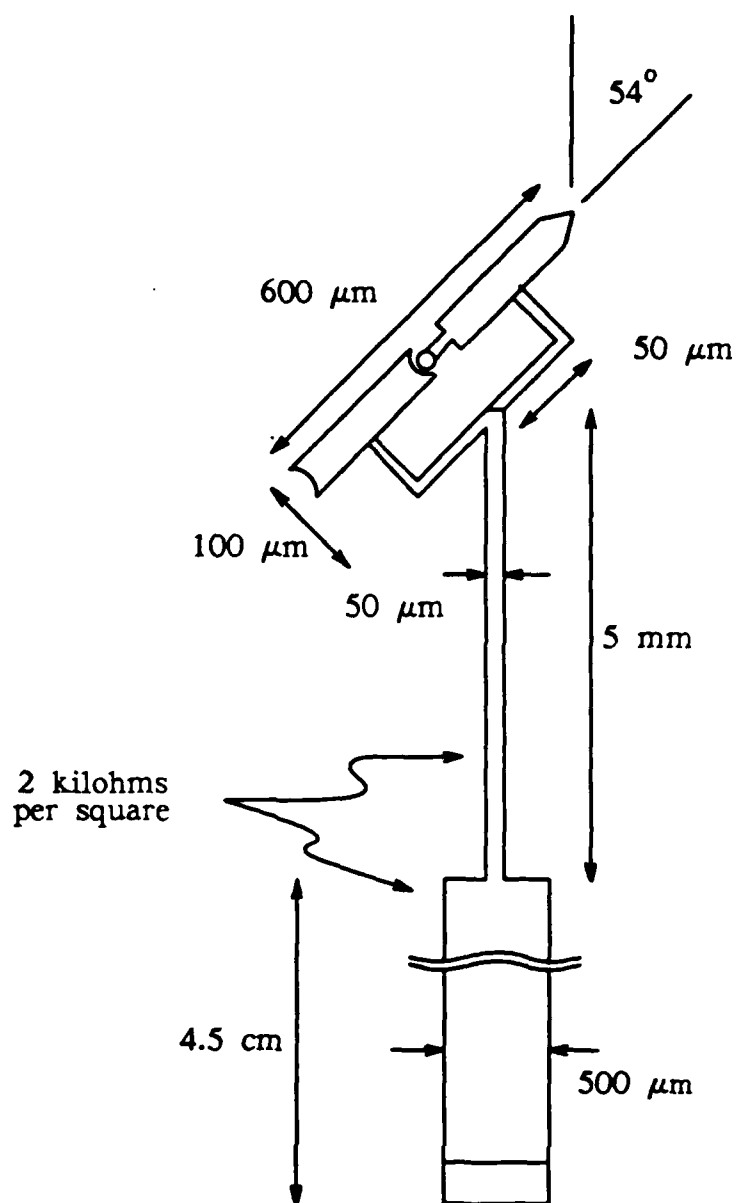
Figure 1.1   E-Field probe design
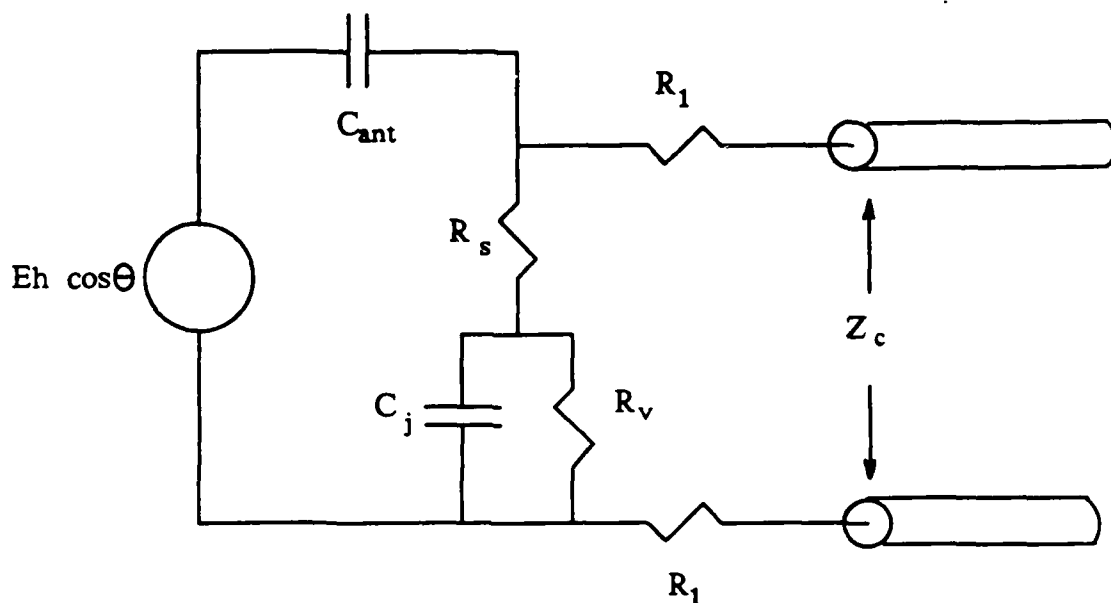
Figure 1.2   AC Model of Probe

the antenna, in addition to being influenced by the permittivity of the material with which the antenna is in intimate contact. This is modeled by $C_{ant}$. The Schottky barrier diode can be modeled by a bulk silicon resistance $R_b$, in series with the parallel combination of the video resistance across the diode depletion region, $R_v$, and the junction capacitance, $C_j$. The video resistance is the inverse slope of the diode's characteristic curve, evaluated at the operating point. Marshburn clarifies that the video resistance is really measured across the leads of the entire diode, which includes the linear bulk resistance $R_b$ in addition to the nonlinear junction resistance [4]. However, since $R_b$ is on the order of 15 ohms, while the nonlinear junction resistance

is somewhere in the kilohm range, the video resistance can be approximated as containing just the nonlinear junction resistance. The junction capacitance is proportional to the charge separation in the depletion region of the diode. Gimpelson proves in his dissertation that the diode actually self-biases with a small negative dc voltage. The resistance $R_1$ is the tab resistance of the transmission line structure across which the diode is mounted. The transmission line is actually two highly resistive leads that are overlayed to provide a large capacitance between them. This capacitance shorts out any ac signal after it propagates a short distance down the transmission line, leaving the dc component (if any) of the signal to reach the end of the transmission line. The impedance looking into the transmission line is called $Z_c$ in Marshburn's work [4]. Both he and Smith [5] use a distributed parameter fields approach in calculating the characteristic impedance of the transmission line. Marshburn takes into account both the unflared and flared portions of the transmission line and calculates that the value of $Z_c$ is approximately 20 kilohms for the probes being manufactured.

Since the time-varying E-field has no dc component, the diode is used to rectify the signal produced across the dipole antenna. Gimpelson completed a simplified modeling and analysis of the dc characteristics of the E-field probe, as a function of the E-field. Marshburn undertook an extensive modeling and analysis of the probe, taking into account noise and frequency effects, which, after a number of assumptions are made, simplifies to the same result that Gimpelson obtained. The complete dc model is shown in figure 1-3 [4]. The nonlinear depletion region of the diode is linearized around the operating
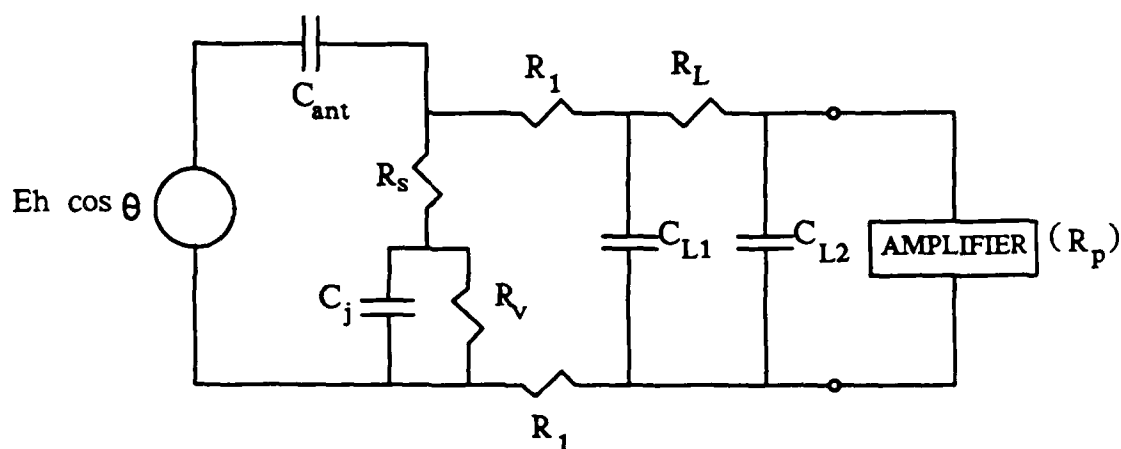
Figure 1.3   Complete DC Model of Probe

point and the diode junction is modeled as a current source in parallel with the video resistance. This model is the simplified dc model and it is the model that Gimpelson derived [2]. It is shown in figure 1-4. $R_T$ is the total dc resistance path. This consists of tracing a path from one side of the diode depletion region, through the diode bulk resistance, through the tab resistance, through the lead resistance, through the amplifier, back through the other lead resistance, back through the other tab resistance, back through the diode bulk region, to the other side of the diode depletion region. This can be traced out in figure 1-3 to satisfy oneself that a complete dc path does exist through the amplifier. Notice that there is no dc path through the dipole antenna section of the model.
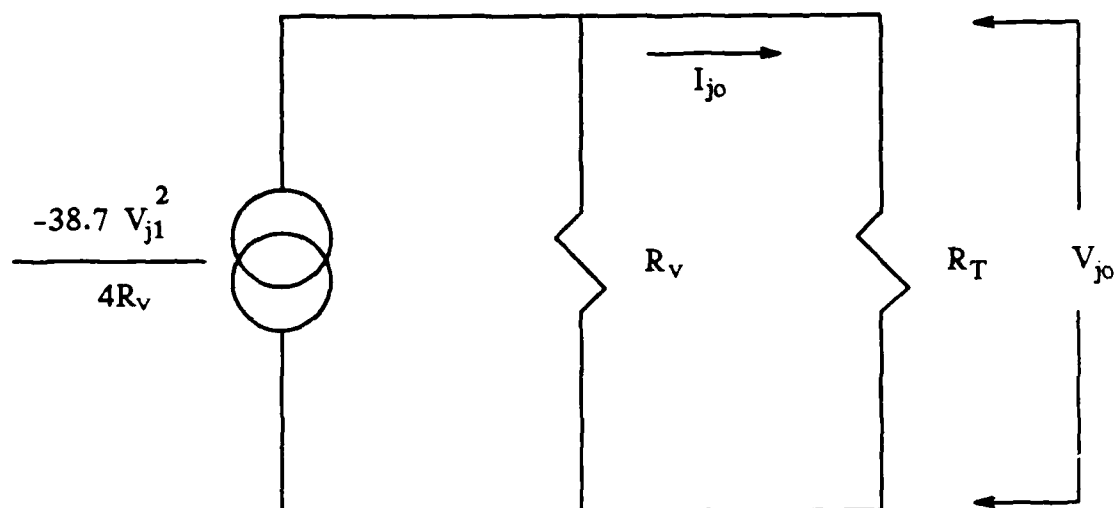
**Figure 1.4**  Simplified DC Model of Probe

Starting with the ideal diode equation,

$$I_j = I_s(e^{\alpha V_j} - 1) \tag{1-1}$$

where $\alpha$ is the reciprocal of the thermal voltage and $I_s$ is the saturation current, Gimpelson expanded the exponential function into a Maclaurin series truncating after three terms. He then let the total voltage term $V_j$ equal a dc term $V_{jo}$ plus a first harmonic $V_{j1}\cos\omega t$. There is some debate over whether the total voltage across the depletion region should be modeled as having only an ac component, since the E-field impinging on the dipole antenna is a pure ac signal, or, as Gimpelson has done, modeled as an ac component, $V_{j1}$, plus a dc component, $V_{jo}$. After carrying out the math, the

difference in the two methods is a constant. This means that both methods will produce the same final result, translating to a difference only in probe sensitivity. Gimpelson's method makes more sense (assuming that the voltage across the diode junction has both an ac and dc component) because, in the steady-state, the voltage across the diode must have both an ac and dc component in order for the probe to work. When the probe is not exposed to an E-field, there is no bias on the probe. This means that the ac and dc component of the voltage across the diode junction is zero. When the probe is exposed to an E-field, the probe will self-bias with a rather fast time constant and there will be both an ac and dc voltage component across the diode junction, which, it must be remembered, is produced as a result of a pure ac signal across the nonlinear diode depletion region. Therefore, the total voltage that Gimpelson used is correct, in the opinion of the author. Substituting this voltage into the current equation and expanding the equation, Gimpelson came up with a cubic equation relating $V_{jo}$ and $V_{ji}$. The complete equation, after expanding out all terms, is a cubic equation in $V_{jo}$ [2]:

$$\frac{\alpha^2}{6}V_{jo}^3 + \frac{\alpha}{2}V_{jo}^2 + (1+\frac{R_v}{R_T}+\frac{\alpha^2}{4}V_{ji}^2)V_{jo} + \frac{\alpha}{4}V_{ji}^2 = 0 \qquad (1\text{-}2)$$

The cubic term equals the squared term when $V_{jo}$ equals $3/\alpha$, or approximately .078 volts. If $V_{jo} << .078$ volts, the cubic term can essentially be ignored and equation 1-2 simplifies to a second order equation. Gimpelson then used the quadratic equation to solve for $V_{jo}$ as a function of $V_{ji}$. His results were as follows [2]:

for $R_v \ll R_T$,

$$V_{jo} = -\frac{\alpha}{4}V_{j1}^2 \qquad (1\text{-}3)$$

for $R_T \ll R_v$,

$$V_{jo} = -\frac{\alpha}{4}(\frac{R_T}{R_v})V_{j1}^2 \qquad (1\text{-}4)$$

As can be seen by both eqns 1-3 and 1-4, $V_{jo}$, which is the dc component of the voltage across the diode's depletion region, is a function of $V_{j1}^2$, which is the squared value of the ac component of the voltage across the diode's depletion region.

As the discussion has now shown, the probe will produce a time-averaged dc signal at the output of the probe connector. To understand what this signal will entail, refer to figure 1-5. Here, the current source in parallel with the video resistance has been replaced by its Thevenin equivalent, and the total resistance, $R_T$, has been broken up into its component resistances. The amplifier will see the voltage across $R_p$ only. $V_{jo}$ can be replaced with the expression in equation 1-3. At this point the dc output of the probe, $V_o$, has been related to $V_{j1}$, the ac component of the voltage across the diode junction. All that remains to do is to relate $V_{j1}$ to the incident E-field on the dipole antenna.

This part of the analysis is where Marshburn and Gimpelson diverge. Referring to figure 1-2, and ignoring the diode bulk resistance, $R_b$, the ac voltage across the diode junction is in reality across the parallel combination
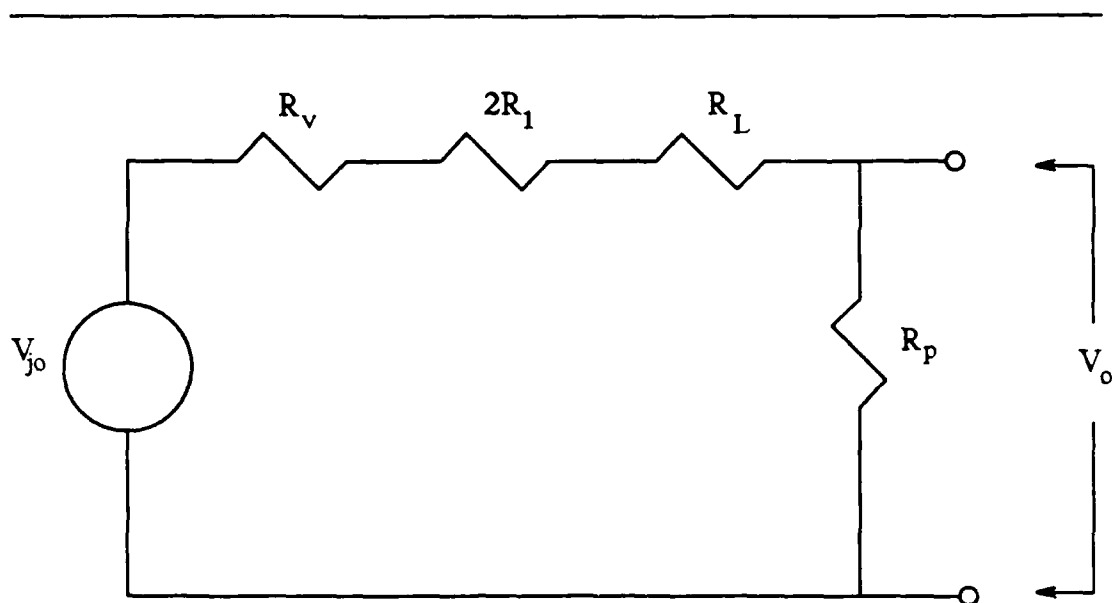
Figure 1.5 DC Model with Component Resistances

of the junction capacitance and video resistance in parallel with the series impedance $2R_1 + Z_c$. This voltage can be referred back, through a voltage divider involving $C_{ant}$, to the dipole excitation Eh $\cos\theta$. Marshburn and Smith carried the full-blown expression back and came up with a huge equation, after all substitutions had been made. This equation relates the final output voltage of the probe back to the impinging E-field. It is a frequency-dependent equation.

Gimpelson, on the other hand, chose to look at figure 1-2 and make comparisons of relative magnitudes of each component of the ac model to see what could be ignored and what would dominate the response. He first ignores $R_b$, as Marshburn and Smith do. He then realizes that the probe is

designed to be used in a frequency band of from 300 MHz to about 18 GHz. In this frequency band, the parallel combination of $C_j$ and $R_v$ will be dominated by $C_j$. Typical values for $R_v$ and $C_j$ are 315 kilohms and .1 picofarads, respectively. Using 1.8 GHz as the operating frequency, $\frac{1}{\omega C_j}$ becomes equivalent to about 884 ohms. At higher operating frequencies this equivalent impedance becomes even lower, which will dominate $R_v$ even more completely. Because of the overlayed lead structure, the transmission line acts as a virtual short to ac signals. $C_j$ is then in parallel with $2R_l + Z_c$, and will dominate this impedance at the frequencies of interest. Gimpelson did an analysis of the required value of $R_l$ in terms of ohms per square needed with the dimensions of the tabs that are currently being manufactured [2]. The two graduate students currently engaged in probe manufacture and improvement make sure that the value of $R_l$ is high enough such that the parallel combination of $2R_l + Z_c$ and $C_j$ is dominated by $C_j$. Taking all of the above simplifications into account, $V_{j1}$ becomes equal to:

$$V_{j1} = Eh \, \cos\theta \left| \frac{C_{ant}}{C_{ant} + C_j} \right| \qquad (1-5)$$

For the dipole antenna that is currently being used, $C_{ant}$ is approximately equal to .0125 picofarads. The output of the probe will appear across the amplifier, not $R_T$, the total dc resistance path, as explained earlier, so the final dc output voltage that should appear across the output connector of the probe, assuming $R_v \ll R_T$, is [2]:

$$V_o = -\frac{\alpha}{4}(Eh\ cos\theta)^2 \left|\frac{V_{j1}}{Eh\ cos\theta}\right|^2 \left(\frac{R_p}{R_b+R_L+2R_1+R_p}\right) \quad (1\text{-}6)$$

or, by substituting eqn 1-5 into eqn 1-6:

$$V_o = -\frac{\alpha}{4}(Eh\ cos\theta)^2 \left|\frac{C_{ant}}{C_{ant}+C_j}\right|^2 \left(\frac{R_p}{R_b+R_L+2R_1+R_p}\right) \quad (1\text{-}7)$$

It must be realized that equation 1-7, which is frequency independant, is a simplification of the full-blown equation that Smith and Marshburn derived. However, Smith and Marshburn's equation simplifies to Gimpelson's equation once numbers are substituted in and values calculated. For the frequency range used in the laboratory, Gimpelson's equation is extremely accurate. These last equations will be used to estimate the value of the E-field once the probe is built and the amplification equipment is designed and built. Notice that the output voltage that appears across the leads of the output connector is a function of the E-field squared. The E-field squared is proportional to the incident power on the probe. So, the dc output voltage of the probe will be proportional to the incident power, or proportional to the value of the incident E-field squared.

## 1.3. Topics of Discussion

This thesis will present information on the analysis and design of amplification and signal conditioning equipment that can be used with the current E-field probes being manufactured. Shielding and grounding techniques, as well as a noise analysis treatment, are central to the design because of the extremely small signal and high output impedance of the

source (probe). Additionally, requirements necessary for a three-axis amplification system will be discussed. Experimental results of the amplifier designed and built will be presented. Finally, the question of whether the probe-amplifier system can be modulated with a low frequency ac signal, followed by using some type of amplification device, such as a lock-in amplifier, to extract the signal from the noise, will be addressed.

# CHAPTER 2

## DESIGN OF A SINGLE AXIS AMPLIFIER

### 2.1. Probe Requirements

The probe places extremely stringent requirements on the type of amplification system chosen. Although Gimpelson [2] has derived formulas for every aspect of probe manufacture, including the magnitude of the lead resistance, there is still a considerable margin for error. The graduate students engaged in probe fabrication have had multiple problems in the manufacturing process. One of the major headaches has been the accurate control of the lead resistance. In order to minimize any effect that changes in the lead resistance might have on the magnitude of the signal reaching the amplifier, it is necessary that the amplifier not load down (draw excessive current from) the source (probe). This means that the input impedance of the amplifier needs to be as large as possible.

Because of the extremely small signal that the probe will be able to generate, the amplifier must be very sensitive to the signal from the probe while rejecting any extraneous signals. This calls for a noise analysis of the system. Noise can be broken up into internal noise and external noise. Internal noise is noise that is generated in any electrical device due to some fundamental processes. An example is thermal noise, which is due to the random motion of electrons in any resistive type device, as long as the

14

temperature of the device is above absolute zero. Internal noise, when referred to the input, will determine the smallest signal that can be detected or amplified by the system. External noise is extraneous signals that impinge on the system somewhere in the signal path and appear in the output, along with the wanted signal. Gimpelson and Marshburn have both completed an internal noise analysis of the probe itself, assuming that the input impedance of the amplifier is infinite. An internal noise analysis of the probe-amplifier system is the subject of chapter 3. Completing an external noise analysis is almost impossible, because this involves taking into account all possible external noise sources in every possible environment that the probe may be operated in. However, some general conclusions may be drawn concerning the configuration of the amplification equipment that will minimize the effect of external noise on the system.

As explained in chapter 1, the output signal of the probe is a dc signal and is related to $V_{jo}$. Therefore, the amplification system must be able to amplify signals down to dc. This means that the dc related parameters of the amplifier need to be controlled so that the signal is not lost in the noise. An example of a problem would be an amplifier with dc offset voltage specifications of 1 millivolt when referred to the input trying to amplify a dc signal voltage of 1 microvolt. The signal would be lost so far down in the noise that even if special filtering or coding techniques were used, the signal may still be indistinguishable from the noise.

## 2.2. Amplifier Design Parameters

Commercially available integrated circuit components were chosen as the most likely solution to the problem. After consulting numerous data books, including National Semiconductor, Motorola, Analog Devices, Intersil and Burr-Brown, a determination was made that an instrumentation amplifier might be the most likely candidate for a front end for the amplifier. This decision was supported by the fact that instrumentation amplifiers, in general, are used in applications where extracting and accurately amplifying low level signals superimposed upon various sized common-mode voltages is desired.

After a data book search, the Burr-Brown INA 110 Fast-Settling FET-Input Very High Accuracy Instrumentation Amplifier was chosen as a building block [6]. Since the actual internal circuitry of the INA 110 is proprietary, a rigorous analysis of some aspects of the INA 110 cannot be done. Figure 2-1 is an INA 110 configuration as used in this design. By connecting A1 and A2 in the noninverting configuration, the input impedance is extremely high. The Burr-Brown data book states that the maximum input current of the amplifier is 50 picoamps [6]. This is due to the extremely small gate current required in a FET. With this sized current requirement, the probe should not have loading problems.

Solving the amplifier configuration for $V_o$, notice that, assuming A1 and A2 are in the linear active region of operation, the voltage potentials on the positive and negative terminals of the input opamps are almost identical. Taking them as identical, the current I is:
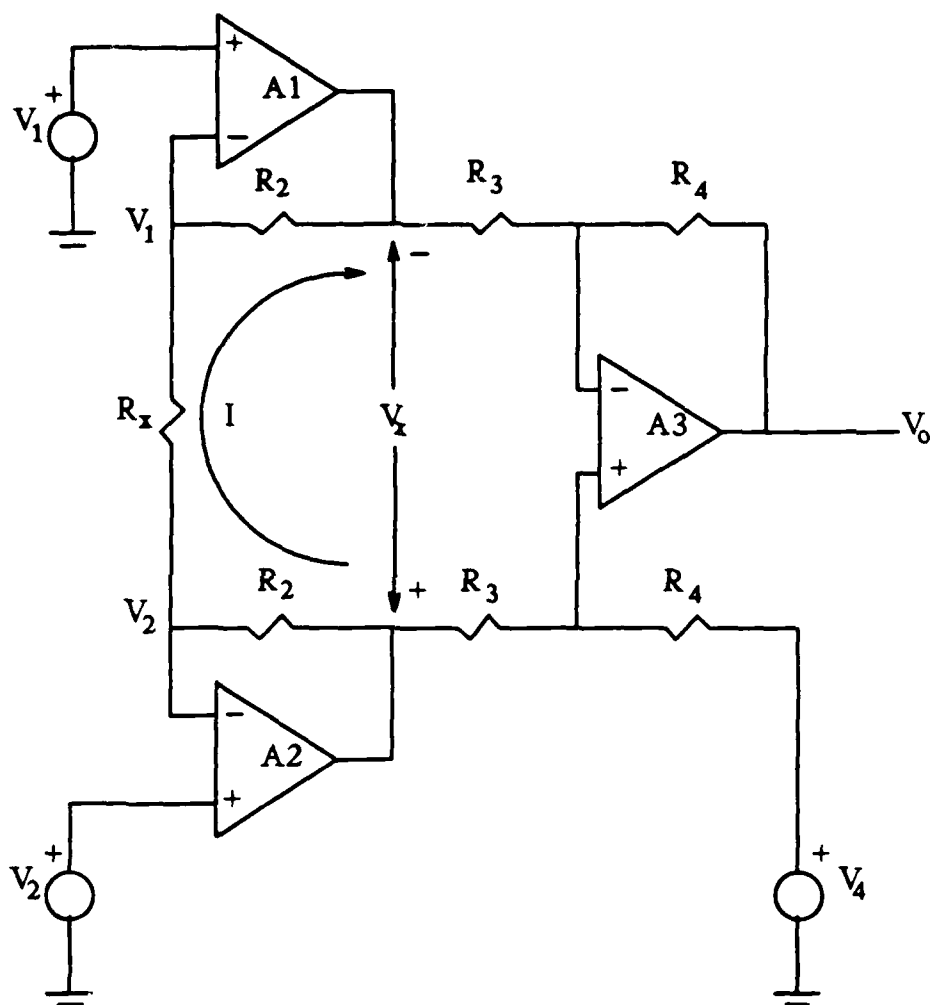
Figure 2.1   INA 110 Configured As Used in Design of Amplifier

$$I = \frac{(V_2 - V_1)}{R_x} \qquad (2-1)$$

This makes $V_x$:

$$V_x = IR = I(R_x + 2R_2) \qquad (2\text{-}2)$$

Therefore:

$$V_x = \left[\frac{V_2 - V_1}{R_x}\right]\left[R_x + 2R_2\right] \qquad (2\text{-}3)$$

Notice that if $V_1 = V_2$, which is a common-mode signal, then there will be no voltage difference across $R_x$. Therefore, no current will flow and $V_x$ will be zero. Budak states that unwanted common-mode signal is introduced into an opamp because the gain from the positive terminal to the output is slightly different in magnitude from the gain from the negative terminal to the output [7]. Theoretically, then, in the particular configuration just analyzed, the common-mode rejection ratio, CMRR, will be infinite because this configuration is perfectly balanced. Practically, though, any imperfections in A1 or A2 or the external resistors will cause a circuit imbalance, which will cause a finite CMRR. Burr-Brown gives the minimum CMRR as 106dB [6], which is very good. This is one of the major criteria that will help reject external noise impinging on the probe.

Taking $V_x$ from figure 2-1 and applying it to figure 2-2, along with $V_4$, $V_o$ can be found. $V_4$ is a voltage that will be used to null the offset, as will be discussed shortly. Using the principle of superposition, along with the fact that the voltage difference between the positive and negative terminals is very small, and taken as negligible, the output voltage is:

$$V_o = \left[\frac{R_4}{R_3}\right]V_x + V_4 \qquad (2\text{-}4)$$
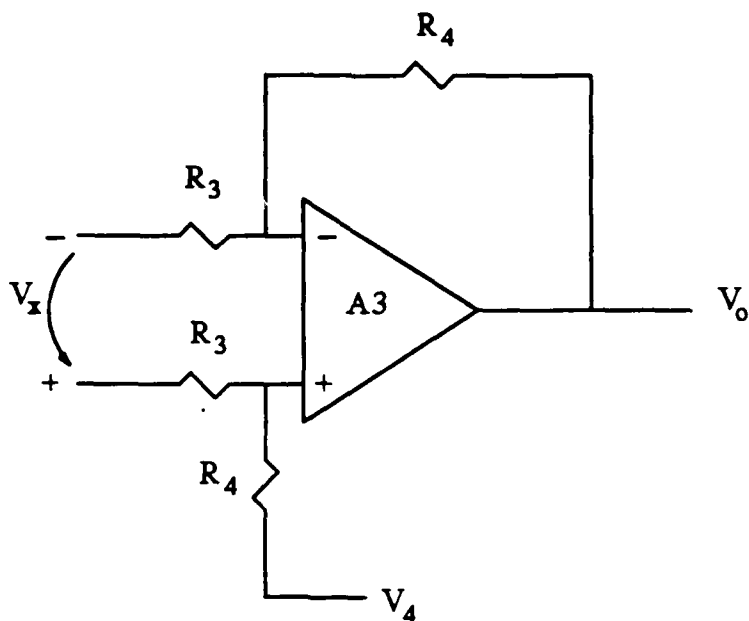
Figure 2.2  Expanded Second Half of INA 110

Therefore, combining equations 2-3 and 2-4:

$$V_o = \left[\frac{V_2 - V_1}{R_x}\right]\left[R_x + 2R_2\right]\left[\frac{R_4}{R_3}\right] + V_4 \qquad (2\text{-}5)$$

In the INA 110, $R_3 = R_4 = 10k$ ohms. These resistors are laser trimmed for extreme accuracy. The final gain equation, using the known resistance values, is:

$$V_o = (V_2 - V_1)\left[1 + \frac{40k}{R_x}\right] + V_4 \qquad (2\text{-}6)$$

By grounding $V_4$, a gain equation can be developed from equation 2-6. For a gain of 500, $R_x = 80.16$ ohms. This is in agreement with Burr-Brown's specifications [6].

As mentioned earlier, a method needs to be developed to control the dc parameters of the amplifier configuration to a close tolerance. Considering the very small voltage signal expected from the probe, controlling the offset voltage is a prime consideration. The specifications for the INA 110 give an offset voltage, referred to the input, of:

$$V_{os} = \left[ 250 + \frac{3000}{\text{Gain}} \right] \quad \text{microvolts} \tag{2-7}$$

Gray & Meyer go through a considerable amount of mathematical calculation to derive the offset voltage of a representative circuit configuration [8]. Unfortunately, the exact configuration must be known. Since that is not true in this case, Burr-Brown's figures cannot be checked for accuracy. Notice that the offset of the second stage, A3, is divided by the gain of the first stage. This is always true, as a rule. Offset voltage is multiplied by the gain of every stage that it passes through, or divided by the gain of every stage it is referred back through. For a gain of 500, $V_{os} = 256$ microvolts. At the output, this is multiplied by 500, which makes the output voltage about 128 millivolts with no input signal applied. By applying a signal, $V_4$, to the amplifier, the offset voltage can be nulled out to a large degree. The accuracy of the nulling depends on the stability of the signal $V_4$. Figure 2-3 is a nulling circuit. Using a very low noise opamp in a unity gain configuration, the best results can be obtained. The dc voltage supply may
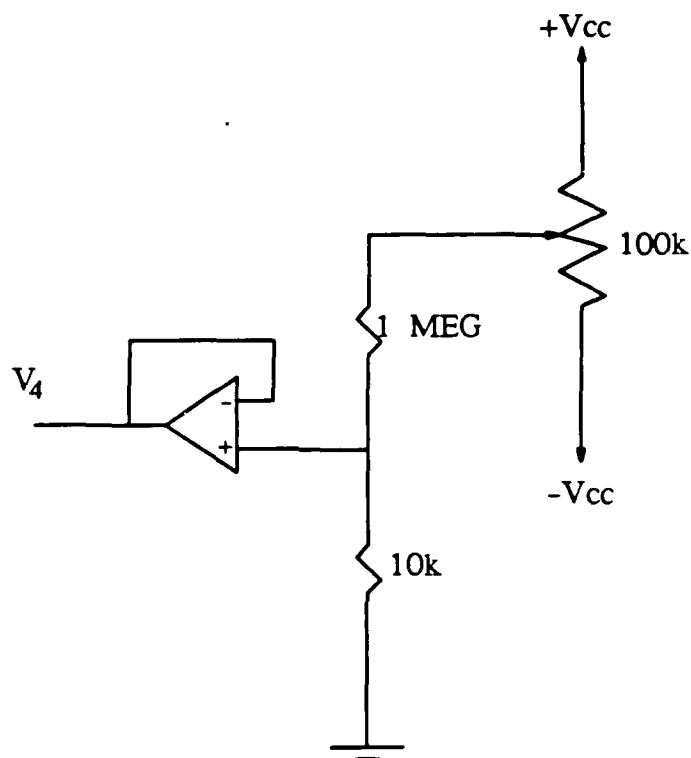
Figure 2.3   Offset Nulling Circuit

affect the nulling circuit over a long time period, as the voltage available at the battery terminals decreases. However, over a period of an hour or so, there will essentially be no effect observed. This is long enough to obtain accurate E-field measurements with the probe. A noise analysis will be done in chapter 3. However, from an intuitive point of view, using the opamp in a unity gain configuration will not multiply any thermal noise generated by the external resistors. As long as the opamp itself does not contribute a

significant amount of noise (hence, use a very low noise opamp), the noise voltage at $V_4$ will be very low and $V_4$ will be a very stable signal to use to null the offset from figure 2-1.

The complete configuration of the first stage of the amplifier is shown in figure 2-4. The two resistors labeled $R_a$ have been added in order for the input FETs to have gate current drive supplied. The values of these resistances, 6.8 megohms, were chosen to minimize noise and maximize the signal from the probe. There is a tradeoff between these two parameters, which will be explained more fully in chapter 3.

A composite gain equation from $V_{jo}$ and from the impinginging E-field can now be derived. Using figures 1-5 and 2-4, $V_2-V_1$ is:
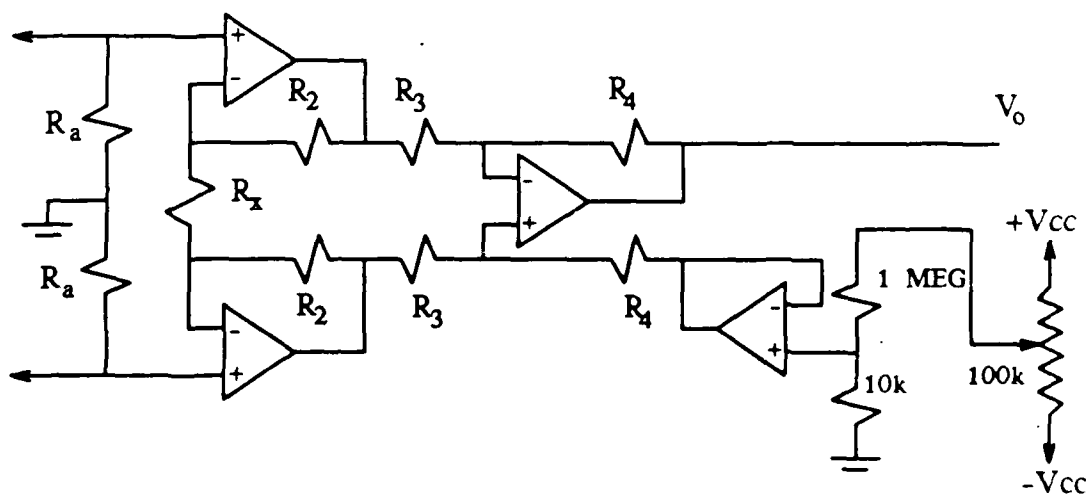


Figure 2.4   Complete First Stage of Amplifier

$$V_2 - V_1 = \left( \frac{13.6}{13.6 + 2R_1 + R_L + R_v} \right) V_{j_0} \qquad (2\text{-}8)$$

The resistance values in the above equation need to be expressed ir megohms. By combining equations 1-7, 2-6 and 2-8, $V_o$ is:

$$V_o = -\frac{\alpha}{4} \left[ Eh \ cos\theta \right]^2 \left[ \frac{C_{ant}}{C_{ant} + C_j} \right]^2 \left[ \frac{13.6}{13.6 + 2R_1 + R_L + R_v} \right] \left[ 1 + \frac{40k}{R_x} \right] + V_4 \qquad (2\text{-}9)$$

This equation is valid for dc and near dc signals. It does not take into account the frequency dependance of the lead structure, as derived by Smith and Marshburn [4,5]. Unless the user is interested in employing some type of modulation technique at other than dc, equation 2-9 will give the output voltage of figure 2-4, connected to a probe, as a function of the impinging E-field. Since we are concerned with dc signals at this point, equation 2-9 is a valid equation.

A low pass filter network was constructed to accomplish two objectives: 1) decrease the external 60 Hz noise visible on the oscilloscope when the system was operating, and 2) decrease the internal noise power spectral density at the output. An active low-pass filter design or band-stop filter design could be used to accomplish the first objective. However, an active design could add internal noise, in the form of thermal, shot, flicker and burst noise to the output of the first stage of the amplifier-filter combination, depending on the internal circuitry of the device or devices used to make the filter an active one. Realizing that the only signals of interest at this time are dc and near dc signals, a passive RC network would probably be superior in terms of internal noise as well as being extremely simple to

construct.    A passive RC filter will essentially add only internal thermal noise to the first stage.

Figure 2-5 is a circuit diagram of the filter. Since 60 Hz noise was the original reason for filtering the output, the RC stages were added one at a time until the noise could no longer be seen on the oscilloscope.   This was needed because the amplifier was not shielded at the time, and was picking up and amplifying an extreme amount of 60 Hz noise.

Solving for the transfer function $\dfrac{V_4}{V_1}$, a matrix equation of the form $[Y][V] = [I]$ can be written.    This is:

$$
\begin{vmatrix}
2G + sC & -G & 0 \\
-G & 2G + sC & -G \\
0 & -G & G + sC
\end{vmatrix}
\begin{vmatrix}
V_2 \\
V_3 \\
V_4
\end{vmatrix}
=
\begin{vmatrix}
GV_1 \\
0 \\
0
\end{vmatrix}
\tag{2-10}
$$

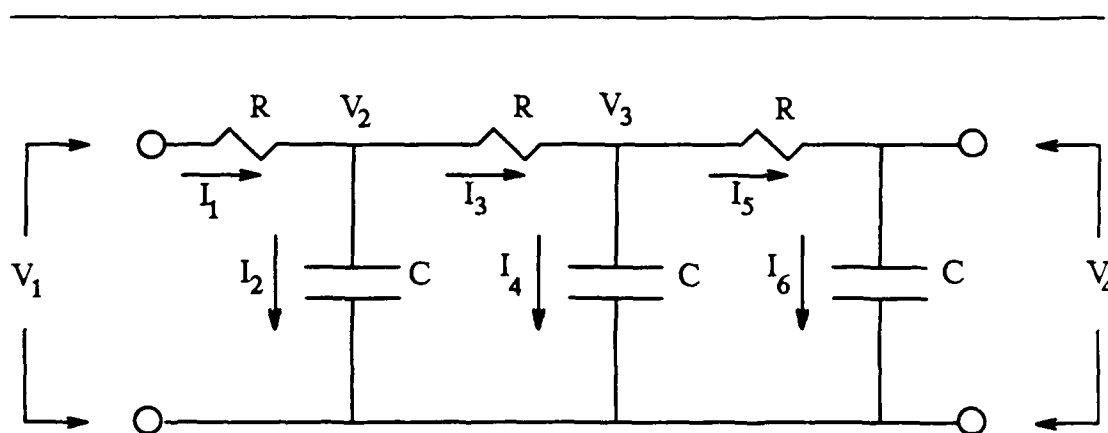After finding $[Y]^{-1}$, the transfer function $\dfrac{V_4}{V_1}$ can be found.    When



Figure 2.5    Three Pole Passive RC Filter

manipulated and reduced, the transfer function becomes:

$$TF(s) = \frac{\left(\frac{1}{R^3C^3}\right)}{s^3 + \left(\frac{5}{RC}\right)s^2 + \left(\frac{6}{R^2C^2}\right)s + \frac{1}{R^3C^3}} \qquad (2\text{-}11)$$

After substituting R = 100k and C = 1 microfarad, equation 2-11 becomes:

$$TF(s) = \frac{1000}{s^3 + 50s^2 + 600s + 1000} \qquad (2\text{-}12)$$

Figure 2-6 is a plot of the magnitude and phase of equation 2-12. The magnitude curve is the darker shaded curve, while the phase curve is the lightly traced curve. Notice the cursor is approximately on the -3dB point of the filter, which occurs at approximately 1.98 rad/sec. Figure 2-7 is the filter with the cursor at the 60 Hz (377 rad/sec) position. Notice that the signal at 60 Hz is down about 95 dB from the maximum value.

The second stage of the amplifier is shown in figure 2-8. This is just a simple noninverting op-amp configuration. This will suffice in terms of offset voltage and internal noise referred to the input, since these factors will be divided by the gain of the first stage when referred back. Nonetheless, an ultra-low noise precision op-amp was used for stage 2. A gain of approximately 20 was achieved. This was about the limit obtainable, without seriously degrading the signal observed at the output on the oscilloscope. This degradation was due to the fact that the first stage can only be nulled out to the limit observable on the oscilloscope at the output of the first stage. The second stage will amplify this essentially unobservable
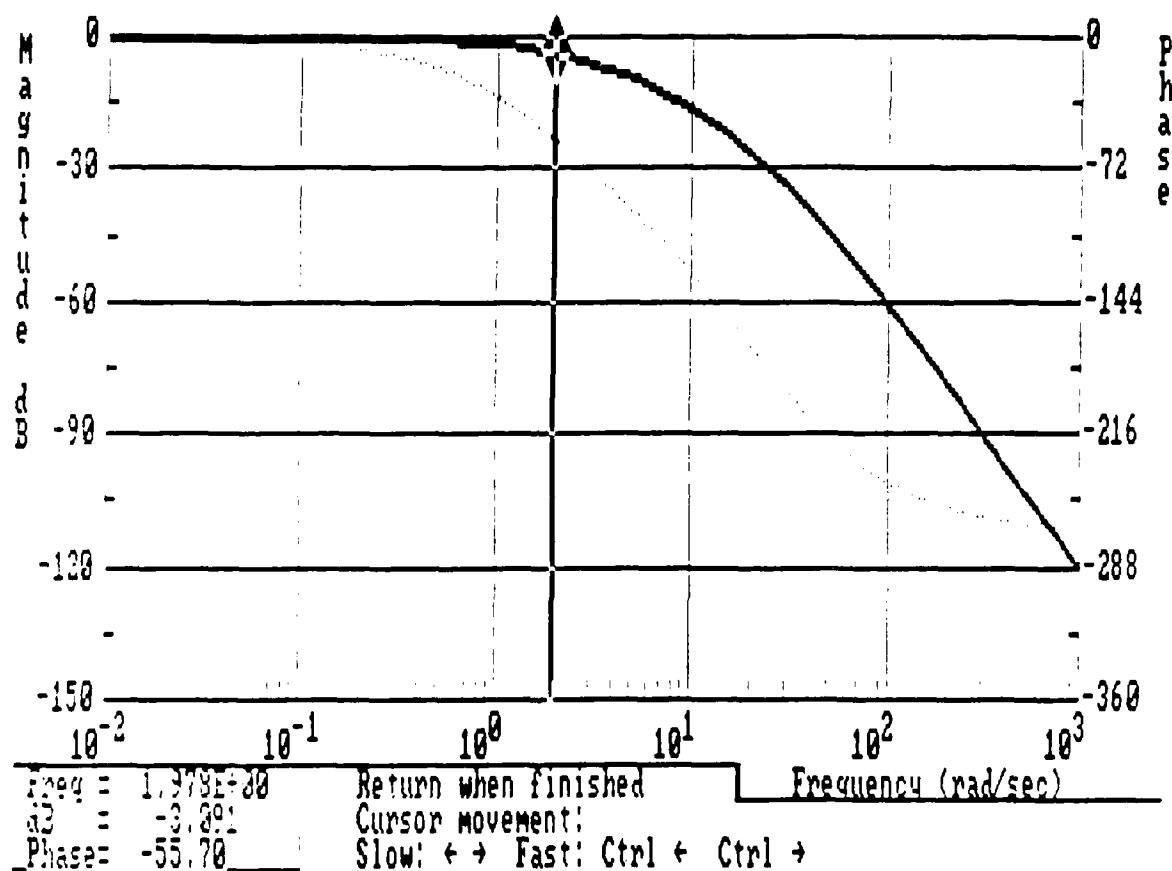
Figure 2.6   Magnitude and Phase Plot of Filter Showing 3dB Point
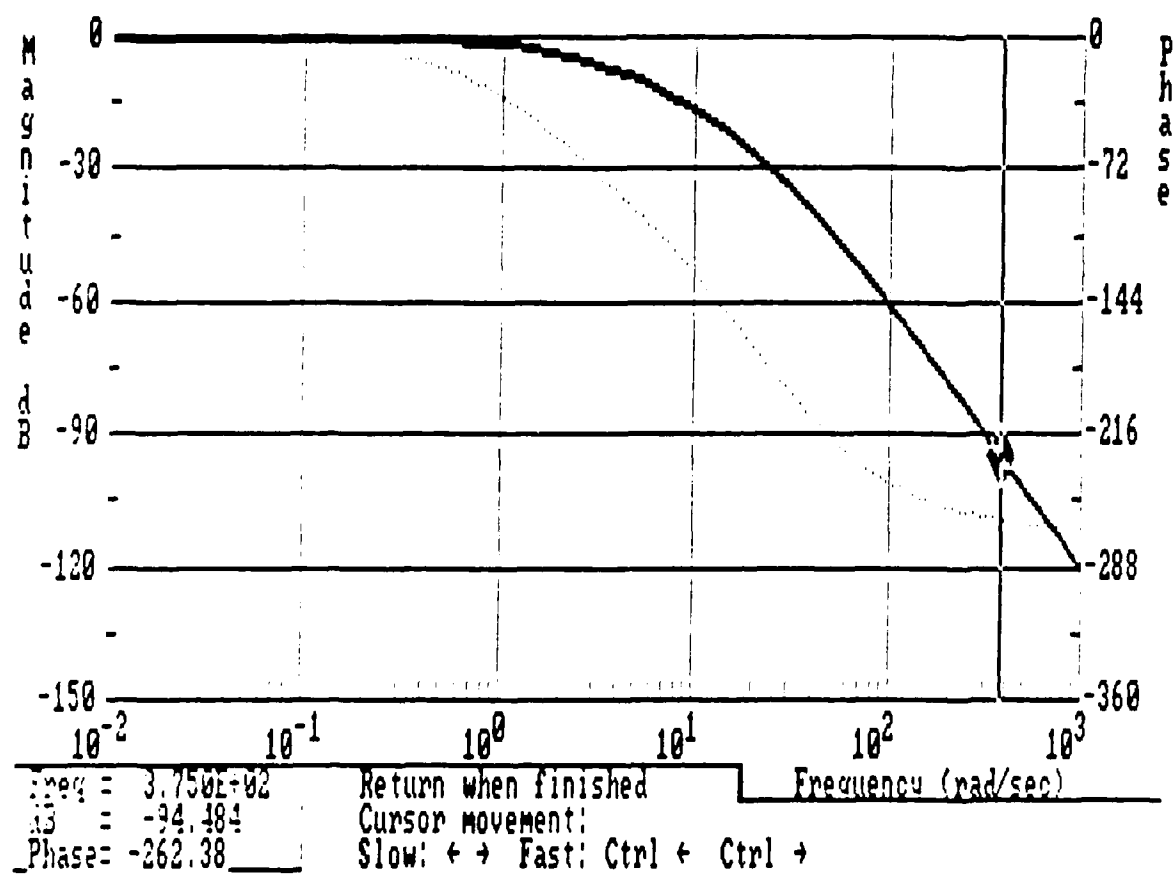
Figure 2.7  Magnitude and Phase Plot of Filter With Cursor at 60Hz
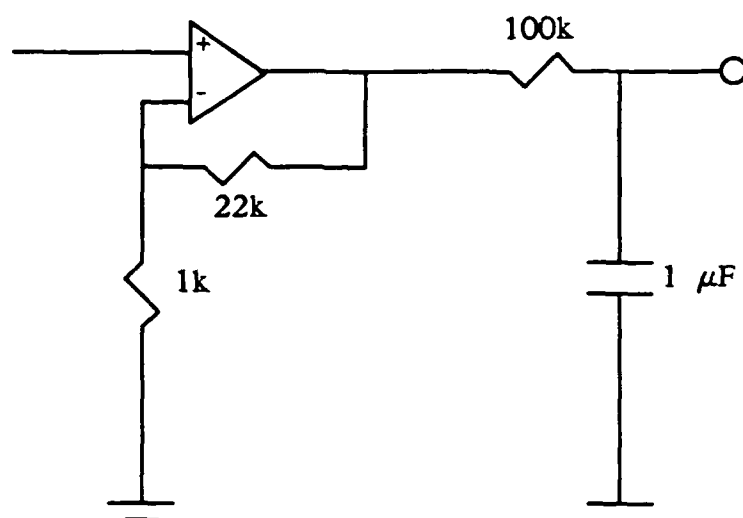
**Figure 2.8**   Second Stage of Amplifier

signal and make it observable at the output of the second stage. This offset and internal noise will add to the offset and internal noise of the second stage, making the signal observed at the output of the second stage fluctuate randomly. An iterative process of nulling the stages one at a time will reduce the error voltage to the minimum possible. This iterative process has to be done after allowing warm-up time to stabilize the temperature drift present when the device is first turned on. Warm-up time of about ten minutes is required, from experimental observation.

Figure 2-9 is the complete amplifier configuration. Notice that the probe is not a grounded source. This can possibly lead to external noise problems, as will be discussed in chapter 3. However, because of the design of the
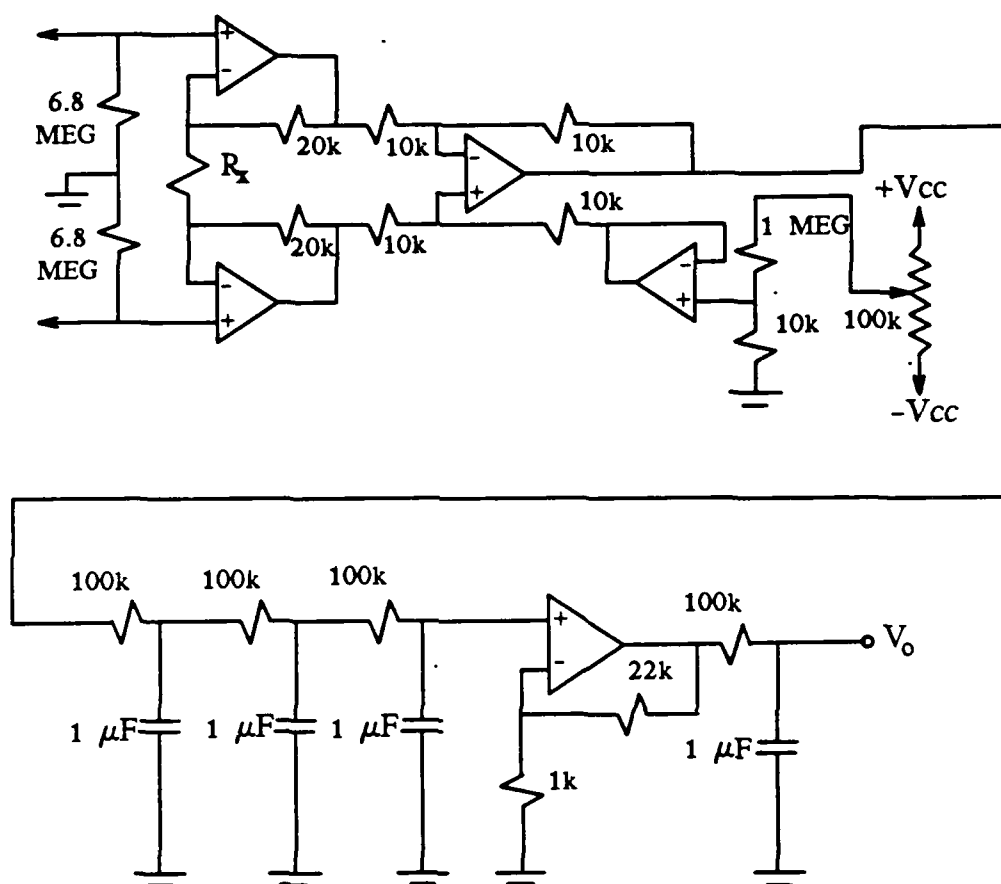
Figure 2.9  Complete Amplifier Configuration for Use With Probe

probe, it is impossible to ground the source, which, it must be remembered,
is actually the diode.   The ground on the oscilloscope is the reference
ground.   The probe is attached directly to the input and a measuring
instrument, such as an oscilloscope or the Keithley electrometer is attached
directly to the output.   In the next chapter, a more thorough analysis of the
performance of this configuration is discussed.

# CHAPTER 3

## ANALYSIS OF PROBE-AMPLIFIER SYSTEM

### 3.1. Introduction

This chapter presents an analysis of the probe-amplifier system discussed in chapters 1 and 2. Internal noise sources are discussed, along with the differences between noise calculations and standard circuit calculations. An internal noise analysis is accomplished, along with a discussion of techniques to minimize external noise. Shielding and grounding are discussed. Finally, a short discussion of a three-axis amplification system, in terms of any special requirements, is presented.

### 3.2. Noise in Systems

Soclof states that the most critical component of an electronic system from the standpoint of the ability of the system to detect weak signals is the first or input stage [9]. This is because it is here that the signal is weakest and therefore most susceptible to noise, either internally generated or externally impinging on the circuit. The ratio of the signal voltage (rms) to the noise voltage (rms) is referred to as the signal-to-noise ratio (SNR). At the input to the first stage of a system, there will be a certain SNR, depending on the signal strength and the external noise level. The internally generated noise in the first stage will add to the noise already present, so

30

that there will generally be a significant degradation of the SNR in the first stage [9]. Even though the signal is amplified by the first stage, so is the noise. Since each successive stage contributes its own internal noise, the SNR actually decreases as the signal passes from one stage to the next. This is why it is so critical to control the noise at the input to the first stage and internal to the first stage.

### 3.3. Sources of Internal Noise

Internal noise generated in integrated circuits is caused by some fundamental physical processes. Gray and Meyer state that internal noise is caused by small current and voltage fluctuations generated within the devices themselves, basically due to the fact that charge is not continuous but is carried in discrete amounts equal to the electron charge [8]. The five basic sources of noise in integrated circuits are shot, thermal, flicker, burst and avalanche noise. Since the probe-amplifier system contains no diodes operating in the Zener region, avalanche noise will not be discussed.

Shot noise is always associated with direct current flow across a potential barrier [10]. More specifically, in integrated circuits with pn junctions, there is a certain carrier concentration at the edge of the depletion region on both sides of the pn junction. Drift and diffusion current flow across the junction, depending on the external voltage across the junction. On a microscopic scale, the passage of each carrier across the junction is a purely random event and is dependent on the carrier having sufficient energy and a velocity directed towards the junction [8]. Since noise is a purely

random signal, in terms of both amplitude and phase, the instantaneous value of the waveform at any given time cannot be determined. However, an average noise power can be measured. This is proportional to the mean square voltage, $\overline{v^2}$, or the mean square current, $\overline{i^2}$ [8,10,11]. For shot noise through a diode, for example, this is given by [9]:

$$\overline{i^2} = 2qI_D\Delta f \qquad\qquad (3\text{-}1)$$

Notice that the power spectral density of equation 3-1, $\dfrac{\overline{i^2}}{\Delta f}$, is constant with respect to frequency. Noise that has a constant power spectral density is known as white noise. The bandwidth, $\Delta f$, is determined by the circuit in which the noise source is acting. Figure 3-1 is a model of shot noise in a diode. The probability density function for the amplitude of shot noise is Gaussian. Bennett proves this through a long argument involving distribution
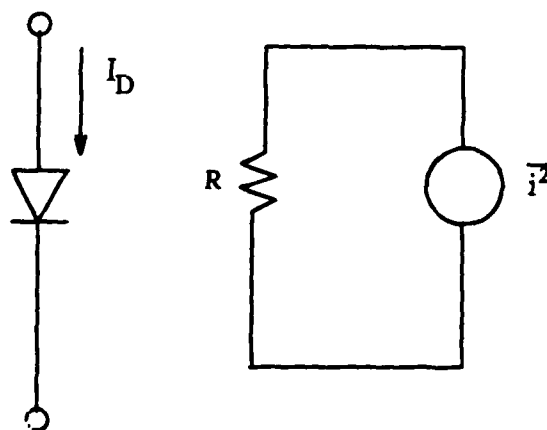


**Figure 3.1**  PN Junction Diode Shot Noise Model

functions and the slope of the distribution function, which is the probability density function. He then uses a statistical theorem, the central limit theorem, which states that the limiting form for the distribution function of the sum of a large number of independent quantities is the Gaussian distribution [11]. The significance of the central limit theorem with respect to noise is the fact that a noise source is often a composite sum of a large number of independent processes [11]. Shot noise, because the current consists of the random arrival of discrete electronic charges, is Gaussian since the total fluctuating current is the sum of a large number of independent pulses. The terms white and Gaussian should not be confused. White refers to the spectral components of the noise having a constant value, while Gaussian refers to the probability density function of the amplitude having a certain form. Additionally, Motchenbacher states that, to a good engineering approximation, common electrical noise lies within plus or minus three times the rms value of the noise wave. The peak-to-peak voltage is less than six times the rms for 99.7% of the time [10]. Interestingly, after speaking to a Burr-Brown engineer on the phone, he stated that their peak-to-peak noise values need to be divided by 6 to obtain rms values. This is necessary to know because some of the Burr-Brown noise figures are listed as peak-to-peak values, and a relationship between peak-to-peak and rms needs to be known. The converted rms values are then squared to obtain mean square values, which, as stated above, are proportional to the average noise power.

Since noise has random phase and is defined solely in terms of its mean square value, it also has no polarity [8]. Any polarity markings on

diagrams are merely used to distinguish a voltage noise generator from a current noise generator.

Thermal noise is generated by a different mechanism than shot noise. It is due to random thermal motion of electrons and is not affected by direct current or absence of direct current. The physical model for thermal noise is derived from the kinetic theory of heat, in the form of Brownian motion of electrons [11]. Bennett goes into a long discussion and derivation of thermal noise, starting with Brownian motion, using the equipartition law of Maxwell and Boltzmann, deriving the definition of noise bandwidth, and finally obtaining an expression for thermal noise [11]. It is directly proportional to the absolute temperature of the material. For a resistor, thermal noise is given by [8,10,11]:

$$\overline{v^2} = 4kTR\Delta f \qquad (3\text{-}2)$$

or, in terms of current:

$$\overline{i^2} = 4kT\frac{1}{R}\Delta f \qquad (3\text{-}3)$$

These equations are derived assuming maximum available power [10,11]. Maximum power can be delivered to a linear constant load circuit when a source is feeding a resistance load equal to its own internal resistance. For complex impedances, ignore all imaginary components. This can be an extremely tedious set of calculations, trying to match each source to each resistance, and if they do not match, trying to figure out the exact available power from each source to each resistance in a network. Consequently,

equations 3-2 and 3-3 will be used, even though impedances are usually not matched. Reactive components do not generate thermal noise, although eddy current losses in inductors and dielectric losses in capacitors can contribute to thermal noise. This thesis will consider all reactive components to be ideal. Notice that thermal noise is also white. Because thermal noise may be considered the superposition of a very large number of random practically independent processes, it satisfies the theoretical conditions for a Gaussian distribution [11]. Thermal noise sources in a resistor can be modeled as shown in figure 3-2. Notice that the current model can be derived from the voltage model by using a Norton equivalent [8]:

$$\overline{i^2} = \frac{\overline{v^2}}{R^2} \qquad (3-4)$$

Thermal noise is a fundamental physical process and is present in any passive resistor, even when no current flows. This means that you may
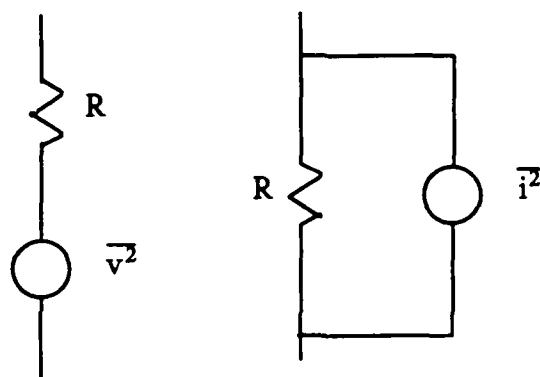


Figure 3.2   Models of Thermal Noise in a Resistor

observe thermal noise without the circuit being activated.

Flicker, or $\frac{1}{f}$ noise is caused, in bipolar transistors, by traps in the silicon lattice, specifically in the emitter-base depletion region, as a result of contamination and crystal defects [8]. It predominates at low frequencies because the time constants, associated with capturing and releasing carriers in the traps described above, are rather long. Flicker noise is always associated with direct current flow, and can be described by [8]:

$$\overline{i^2} = K_1 \left| \frac{I^a}{f^b} \right| \Delta f \tag{3-5}$$

where $K_1$ is a constant for a particular device that has to be experimentally determined after the chip is manufactured. It can vary by orders of magnitude, even on the same wafer, due to the variation of contamination and crystal defects across the wafer [8]. This makes flicker noise very difficult to accurately predict and control. I is a direct current, which is a bias current for the particular device or junction in question. The constants a and b are somewhere around unity. Notice that flicker noise varies inversely with frequency. This makes it predominate at low frequencies, which is the range that the probe-amplifier system operates in.

Burst noise is another type of low-frequency noise found in integrated circuits. It is related to heavy-metal ion contamination [8]. Burst noise can occur with multiple time constants. This will produce "multiple bumps" on a power spectral density vs frequency plot. Because it is related to wafer contamination levels, it is also very difficult to predict and control. It can

be described by [8]:

$$\overline{i^2} = K_2 \left| \frac{I^c}{\left[1 + \left[\frac{f}{f_c}\right]^2\right]^2} \right| \Delta f \qquad (3\text{-}6)$$

where $K_2$ is a constant that is related to the contamination level for a particular wafer. I is a direct current, just as in $\frac{1}{f}$ noise. The constant c is about unity. The frequency $f_c$ is a cutoff frequency. There will not be much use made of burst noise in the following analysis, due to the difficulty of characterization. It was included for completeness.

## 3.4. Noise Bandwidth

Noise bandwidth is not the same as the commonly used 3 dB bandwidth. There is one definition of bandwidth for the signal and another definition of bandwidth for the noise. The bandwidth for the signal is defined as the frequency separation between the half power points. This is assuming that you have an amplifier or some type of tuned circuit, so that you can determine the maximum response and calculate the half power points from there.

The noise bandwidth, $\Delta f$, is defined as the frequency span of a rectangularly shaped power gain curve equal in area to the area of the actual power gain vs frequency curve [10]. In equation form [10]:

$$\Delta f = \frac{1}{G_0} \int_0^\infty G(f)\, df \qquad (3\text{-}7)$$

$\Delta f$ is the noise bandwidth in Hz. $G_0$ is the peak power gain. $G(f)$ is the power gain as a function of frequency. Since power gain is proportional to voltage gain squared, equation 3-7 can be rewritten as:

$$\Delta f = \frac{1}{A_0^2} \int_0^\infty A(f)^2\, df \qquad (3\text{-}8)$$

As can be seen here, if $A(f)^2$ is not a simple function of frequency, the integral may not be easy to solve. Figure 3-3 is a representative pictorial of equation 3-8. Bennett , Motchenbacher and Buckingham all say that one is usually forced into a graphical integration approach [10,11,12]. Graphical integration is very tedious unless the function is very simple. There is an
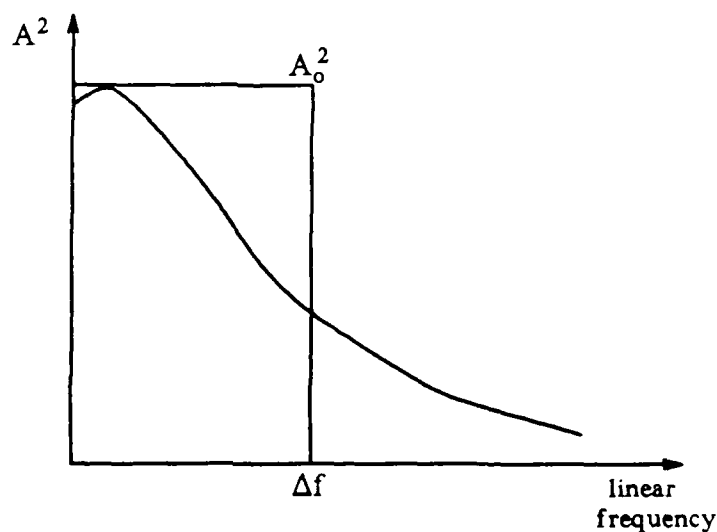


Figure 3.3  Illustration of Noise Bandwidth

alternative that is accurate enough for purposes of this thesis. A simple RC filter frequency response falls off at 6 dB/octave. $\nabla f$ is then 1.57 times the cutoff frequency. As more poles are added at the same cutoff frequency, $\Delta f$ approaches the cutoff frequency. For a three pole filter configuration, such as the one used for the probe-amplifier system, with poles not all coincident (poles are at -1.98, -15.55 and -32.47 rad/sec), $\Delta f$ is very close to 1.57 times the -3 dB point of the filter. Therefore, taking the results of the -3 dB bandwidth from chapter 2, the noise bandwidth will be taken as 3.1 rad/sec. This is a good engineering approximation.

## 3.5. Circuit Noise Calculations

When sinusoidal signal voltage sources of the same frequency and amplitude are connected in series, the resultant voltage has twice the common amplitude if they are in phase, and combined they can deliver four times the power of one source. If, on the other hand, they are out of phase by 180 degrees, the net voltage and power is zero [10]. For other phase conditions, phasor algebra can be used.

If two sinusoidal signal voltage sources of different frequencies with rms amplitudes $V_1$ and $V_2$ are connected in series, the resultant voltage has rms amplitude equal to $\left[V_1^2 + V_2^2\right]^{1/2}$. The mean square value of the resultant voltage, $V_r^2$, is the sum of the mean square values of the components [10].

Noise is a purely random signal, in terms of amplitude and phase, as stated at the beginning of this chapter. Equivalent noise generators, which we somehow would like to use for circuit calculations, represent a very large

number of component frequencies with a random distribution of amplitudes and phases. When independent noise generators are connected in series, the output power is the sum of the separate output powers, and consequently it is valid to combine the mean square values of the sources to obtain a resultant mean square value, as stated in the paragraph above. This statement applies to noise current sources in parallel [8,10]. As Gray and Meyer state, the only information available for use in circuit calculations concerns the mean square value of the signal [8].

Each separate resistor, diode, transistor, etc., can be modeled using basic modeling techniques. If each component is then analyzed on the basis of the model, independent noise sources can be added to the model to take into account the fundamental sources of noise already enumerated. Resistors can be modeled as an ideal resistor, in series with a thermal mean square voltage source or in parallel with a thermal mean square current source. The transistor can be modeled by adding thermal noise sources to all bulk resistances, a shot noise source to the collector current, (because of the reversed biased pn junction between the collector and base regions), and shot noise, $\frac{1}{f}$ noise, and burst noise sources to the base current (to take into account the emitter-base junction). All of these sources are independent because they are all caused by independent physical phenomena. An entire system can be modeled this way, component by component. If this were done, the principle of superposition could be used, and the mean square value of the output noise would be the sums of the mean square values of all the independent noise sources, just as if these noise sources were

independent external excitations on an ideal noiseless system. However, except for the most simple systems, the calculations required to determine the total output noise would quickly proliferate. To complete a noise analysis on a single opamp would be a monumental task.

In the above discussion, the sources were said to be independent. Another term for this is uncorrelated. If the signals are partially or fully correlated, then the mean square of the resultant voltage is not just equal to the sum of the mean square values of the two signals, but is equal to [10]:

$$V_r^2 = V_1^2 + V_2^2 + 2\rho V_1 V_2 \qquad (3-9)$$

The term $\rho$ is called the correlation coefficient. It can range from -1 to 1. When $\rho = 0$ the voltages are uncorrelated. When $\rho = 1$ the voltages are totally correlated. When $\rho = -1$ this implies subtraction of correlated signals, and the signals are 180 degrees out of phase [10].

The reason that correlation is important is because there has to be a more manageable way to analyze a system without modeling the noise sources in every component and performing all of the required calculations. This is where a noise model for a two-port network is used. Before discussing such a model, and relating it to the probe-amplifier system discussed in chapter 2, it is important to understand the basis for its use.

One of the major reasons for going to a two-port parameter approach is to find equivalent input mean square voltage and current generators, $\overline{v_i^2}$ and $\overline{i_i^2}$. These can be compared to the input signal, which will allow one to be able to determine whether or not the signal will be able to be distinguished

from the noise. Most noise books define all kinds of figures of merit to compare signals and noise. There are noise figures and noise factors and noise temperatures and noise resistances. The only standard that will be used in this thesis is to say that a SNR of one at the input to the amplifier will be used as the minimum detectable signal.

When a two-port parameter approach is used to consolidate multiple independent noise sources together, both an equivalent input mean square voltage generator and current generator must be used in the model. Gray and Meyer present a nonrigorous but very intuitively appealing argument concerning why this must be so [8]. Consider figure 3-4. If $R_s$ equals zero, $\overline{i_i^2}$ is shorted out. Since the original circuit will still have output noise, $\overline{v_i^2}$ is necessary to represent this behavior. If $R_s$ is infinite, $\overline{v_i^2}$ is effectively nulled out. In this case, $\overline{i_i^2}$ is necessary to represent the actual circuit behavior [8]. In these cases, the correlation coefficient will be zero. If $R_s$ is finite the correlation coefficient may have to be taken into account. However, if either $\overline{v_i^2}$ or $\overline{i_i^2}$ dominates, the correlation coefficient can be ignored, which
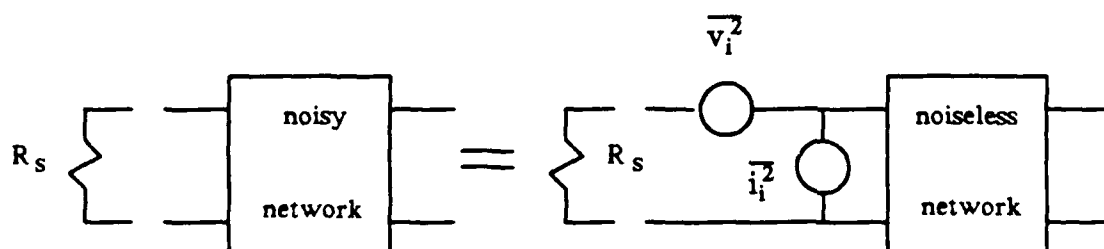


**Figure 3.4** Equivalent Input Noise Generators for a Two-Port Network

greatly simplifies the math. Additionally, if the source resistance is very small, $\overline{i_i^2}$ will be almost shorted out, so it can be effectively ignored. The same holds for $\overline{v_i^2}$ if the source resistance is very large.

By putting the concepts of the last few paragraphs together, it becomes apparent that when a two-port parameter approach with $\overline{v_i^2}$ and $\overline{i_i^2}$ are used to represent a system that would otherwise be prohibitively complicated to solve, correlation between $\overline{v_i^2}$ and $\overline{i_i^2}$ is a possibility, and equation 3-9 may have to be used.

### 3.6. A Noise Model for an Amplifier System

In an amplification system, when noise is referred to the input, it is divided by the gain of every stage that it is referred back through. In an opamp, for instance, the first stage determines the noise behavior almost exclusively, assuming that it has both voltage gain and current gain [8]. It is therefore most important to have an accurate model of the first stage of the amplifier. Grey and Meyer present an excellent treatment of a very specific FET input noise model for a two-port network. Unfortunately, the engineers at Burr-Brown could not give out the bias specifications or whether active loading was used or even the specific manufacturer's number of the FETs used in the input stage of the INA 110.

Motchenbacher [10] presents a very general noise model that can be used with any linear two-port network. This noise model will have to be used, due to the unavailability of data concerning the exact circuit configuration, as stated above. Motchenbacher's noise model is depicted in figure 3-5. It has

been modified slightly for purposes of this thesis. $\overline{v_{R_s}^2}$ is the thermal noise of the source resistance, $R_s$. $\overline{v_i^2}$ and $\overline{i_i^2}$ are the equivalent input noise generators. $\overline{v_{on}^2}$ is the output noise of the system. $V_s$ is the source and $V_o$ is the output signal. $Z_i$ is the input impedance of the system. $A_v$ is a noise free amplifier gain. The goal of the model is to represent all of the noise sources as one equivalent input noise generator, referred back to the signal source, that can be compared to the signal source, $V_s$. This total equivalent input noise generator will be called $\overline{v_{tin}^2}$.

Since noise is being calculated, mean square values have to be used. Using basic circuit principles and ignoring correlation for the moment, $\overline{v_{on}^2}$ is:

$$\overline{v_{on}^2} = A_v^2 \left| \frac{(\overline{v_i^2} + \overline{v_{R_s}^2})Z_i^2}{(R_s+Z_i)^2} + \frac{\overline{i_i^2}Z_i^2R_s^2}{(R_s+Z_i)^2} \right| \quad (3\text{-}10)$$

The transfer function from $V_s$ to $V_o$ is called the system gain, K. Therefore, $K = \dfrac{V_o}{V_s}$. K is not to be confused with $A_v$. $A_v$ is only the gain of the
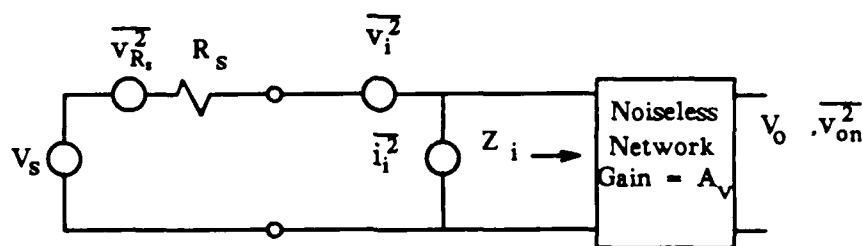


Figure 3.5    Amplifier Noise Model With Signal Source

amplifier, whereas K represents gain all the way back to the signal source, $V_s$. Expressing the output signal voltage in terms of the input signal source:

$$V_o = \frac{A_v Z_i}{R_s + Z_i} V_s \tag{3-11}$$

Therefore, K is:

$$K = \frac{A_v Z_i}{R_s + Z_i} \tag{3-12}$$

The total output noise divided by the system gain gives an expression for the total equivalent input noise referred back to the signal source.

$$\overline{v_{tin}^2} = \frac{\overline{v_{on}^2}}{K^2} \tag{3-13}$$

Therefore, combining equations 3-10, 3-12 and 3-13, the total equivalent input noise, $\overline{v_{tin}^2}$ is:

$$\overline{v_{tin}^2} = \overline{v_{R_s}^2} + \overline{v_i^2} + \overline{i_i^2} R_s^2 \tag{3-14}$$

As mentioned previously, the equivalent input voltage and current generators will probably not be independent, since they are composite values, referred to the input, of actual noise mechanisms. To take this into account, equation 3-14 is modified as follows:

$$\overline{v_{tin}^2} = \overline{v_{R_s}^2} + \overline{v_i^2} + \overline{i_i^2} R_s^2 + 2\rho v_i i_i R_s \tag{3-15}$$

This equation can be applied to any two-port network to determine the total equivalent input noise.

## 3.7. Noise Analysis of the Probe-Amplifier System

Gimpelson [2] did a noise analysis of the probe by itself, assuming an ideal noiseless, infinite impedance amplifier. In this analysis he went through a considerable amount of effort to model the transmission line. I will just use his results, without rederiving them, in the overall scheme of modeling the system. Figure 3-6 is a noise model of the entire system. Starting on the left, the signal source is $\frac{V_{jo}}{R_v}$, and is labeled $I_s$. This relates back to figure 1-4. $R_v$ is the diode video resistance and its noise source is $\overline{i_{R_v}^2}$. Gimpelson [2] modeled the transmission line and ended up with a frequency dependent resistor, $R(\omega)$, and a capacitance, $2C$, where $C$ is the capacitance of the transmission line. $R(\omega)$ is equal to, from Gimpelson [2], $\frac{1}{R_L(\omega C)^2}$. $R(\omega)$ has a noise source associated with it, $\overline{i_{R(\omega)}^2}$. As stated earlier, energy storage
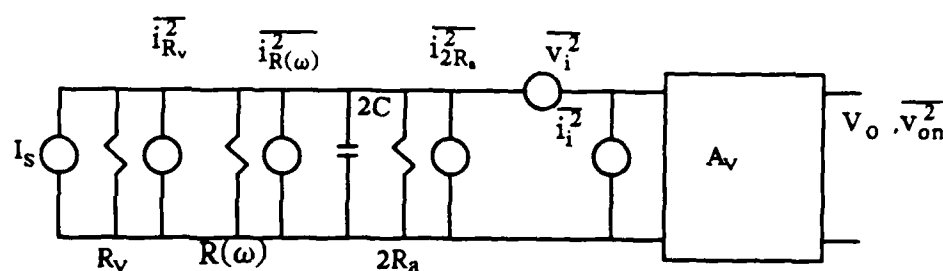


Figure 3.6   Noise Model of Probe-Amplifier System

elements will be taken as ideal, so the capacitance has no noise source associated with it. The other elements come from the amplifier. $2R_a$ is the combination of resistors used to supply the FET input current drive, along with its noise source, $\overline{i_{2R_a}^2}$. $\overline{v_i^2}$ and $\overline{i_i^2}$ come from the model given in the previous section. $A_v$ is $1+\dfrac{40k}{R_x}$ and is equal to 500.

Using the principles discussed in the previous sections of this thesis, $\overline{v_{on}^2}$ is:

$$\overline{v_{on}^2} = \left|1+\frac{40k}{R_x}\right|^2 \frac{\left[\overline{i_{R_v}^2}+\overline{i_{R(\omega)}^2}+\overline{i_{2R_a}^2}+\overline{i_i^2}\right]\left|R_v||R(\omega)||2R_a||\dfrac{2}{\omega C}\right|^2 Z_i^2}{\left|Z_i + \left|R_v||R(\omega)||2R_a||\dfrac{2}{\omega C}\right|\right|^2}$$

$$+ \left|1+\frac{40k}{R_x}\right|^2 \frac{Z_i^2\overline{v_i^2}}{\left|Z_i + \left|R_v||R(\omega)||2R_a||\dfrac{2}{\omega C}\right|\right|^2} \tag{3-16}$$

The transfer function $\dfrac{V_o}{I_s}$, where $I_s$ is equal to $\dfrac{V_{jo}}{R_v}$, is:

$$V_o = \left|\frac{13.6R_v}{13.6+2R_1+R_L+R_v}\right|\left|1+\frac{40k}{R_x}\right| I_s \tag{3-17}$$

where the 13.6 is in megohms. The total equivalent input voltage noise, $\overline{v_{tin}^2}$, is equal to $\dfrac{\overline{v_{on}^2}}{K^2}$. The total equivalent input noise current, $\overline{i_{tin}^2}$, is $\dfrac{\overline{v_{tin}^2}}{R_v^2}$. This is:

$$\overline{i_{tin}^2} = \frac{\left[\overline{i_{R_v}^2} + \overline{i_{R(\omega)}^2} + \overline{i_{2R_a}^2} + \overline{i_i^2}\right]\left|R_v||R(\omega)||2R_a||\frac{2}{\omega C}\right|^2 Z_i^2\left(13.6 + 2R_1 + R_L + R_v\right)^2}{\left|Z_i + \left[R_v||R(\omega)||2R_a||\frac{2}{\omega C}\right]\right|^2 \left(13.6R_v\right)^2}$$

$$+ \frac{Z_i^2\overline{v_i^2}\left(13.6 + 2R_1 + R_L + R_v\right)^2}{\left|Z_i + \left[R_v||R(\omega)||2R_a||\frac{2}{\omega C}\right]\right|^2 \left(13.6R_v\right)^2} \tag{3-18}$$

Taking correlation into account, equation 3-18 becomes:

$$\overline{i_{tin}^2} = \frac{\left[\overline{i_{R_v}^2} + \overline{i_{R(\omega)}^2} + \overline{i_{2R_a}^2} + \overline{i_i^2}\right]\left|R_v||R(\omega)||2R_a||\frac{2}{\omega C}\right|^2 Z_i^2\left(13.6 + 2R_1 + R_L + R_v\right)^2}{\left|Z_i + \left[R_v||R(\omega)||2R_a||\frac{2}{\omega C}\right]\right|^2 \left(13.6R_v\right)^2}$$

$$+ \frac{Z_i^2\overline{v_i^2}\left(13.6 + 2R_1 + R_L + R_v\right)^2}{\left|Z_i + \left[R_v||R(\omega)||2R_a||\frac{2}{\omega C}\right]\right|^2 \left(13.6R_v\right)^2} \tag{3-19}$$

$$+ \frac{2\rho i_i v_i\left|R_v||R(\omega)||2R_a||\frac{2}{\omega C}\right| Z_i^2\left(13.6 + 2R_1 + R_L + R_v\right)^2}{\left|Z_i + \left[R_v||R(\omega)||2R_a||\frac{2}{\omega C}\right]\right|^2 \left(13.6R_v\right)^2}$$

Equation 3-19 is the expression that needs to be compared to the signal, $I_s$, to determine the minimum detectable signal, using a signal to noise ratio of one. Values for the terms in equation 3-19 are:

$\Delta f = 0.49$ Hz

$R_L = 8$ Megohms

$C = 0.5$ nF

$2R_a$ = 13.6 Megohms

$Z_i$ = $2 \times 10^{12}$ ohms

$R_v$ = 315 kohms

$R(\omega)$ = $3.2 \times 10^7$ ohms, from the equation that Gimpelson derived using 8 Megohms for the lead resistance. The $\omega$ value that is used to compute $R(\omega)$ is the lead resistance bandwidth, which is $\frac{1}{4\pi R_L C}$. This formula was derived by Smith [5] using a distributed parameters approach, as mentioned in chapter 1. This value of $\omega$ is 125 rad/sec which is only used to compute the magnitude of $R(\omega)$. To compute $\overline{i^2_{R(\omega)}}$, the noise bandwidth must still be used.

$\overline{i^2_{R_v}}$ = $2.6 \times 10^{-26}$ $A^2$

$\overline{i^2_{2R_a}}$ = $6.0 \times 10^{-28}$ $A^2$

$\overline{i^2_{R(\omega)}}$ = $2.54 \times 10^{-28}$ $A^2$

$\overline{i^2_i}$ = $3.2 \times 10^{-30}$ $A^2$

$R_1$ = 400 kohms

$\overline{v^2_i}$ = $1 \times 10^{-16}$ $V^2$

$\rho$ = 1, which will give the worst case noise figures. This assumes total correlation between $\overline{v^2_i}$ and $\overline{i^2_i}$.

Most of these values have been mentioned or derived before. $\Delta f$ is derived from dividing the noise bandwidth by $2\pi$. C was calculated using the probes that are currently being manufactured. $R_L$ is a value chosen based upon lab experience. One of the graduate students engaged in probe manufacture claims that a value of 2 megohms is achievable, but no probes

that were ever measured in the lab had a lead resistance near 2 megohms.
The mean square noise values were calculated using the formulas presented
in the earlier part of this chapter. Equation 3-19 can be evaluated directly.
When this is done, $\overline{i_{tin}^2}$ is equal to $7.20 \times 10^{-26}$ A$^2$. Converting this to an rms
value by taking the square root, $i_{tin}$ is equal to 0.27 picoamps. As an aside,
the value of the correlation term in equation 3-19 is $3.04 \times 10^{-28}$ A$^2$, which is
small compared to the other terms. However, it was included in order to
make sure that the calculations were as accurate as possible. The signal $I_s$ is
derived from the impinging E-field. Equating the signal value from chapter
1 to the theoretical noise value, which is a SNR of one, the theoretical
minimum E-field that can be distinguished from the noise can be calculated:

$$\frac{\alpha}{4R_v}E^2 h^2 \left| \frac{C_{ant}}{C_{ant}+C_j} \right|^2 = 2.7 \times 10^{-13} \qquad (3\text{-}20)$$

This equation assumes that $\cos\theta$ is one, which means that the dipole and the
E-field are parallel. Solving for the minimum E-field, a value of 2.8
volts/meter is found. This value is very close to the value that Gimpelson
calculated, which was 4.5 volts/meter. However, Gimpelson used the
bandwidth of the probe transmission line. The bandwidth used for the
calculations in this thesis was 0.49 Hz, which, as mentioned before, is the
noise bandwidth of the system, as calculated in the noise bandwidth section.
This significantly reduces the noise, which will allow measurement of a
theoretically smaller E-field (although not much smaller) even after adding
amplifier noise (Gimpelson assumed a perfect amplifier in his analysis).

After examining equation 3-19 in detail, the biggest noise contributer is the diode itself. The next largest contributer is the resistance used to supply gate current drive to the FETs. As mentioned previously, these resistors are 6.8 megohms each. The larger these resistors are made, the more gain that can be achieved, which can be seen by examining equation 2-9. However, the larger these resistors are, the more thermal noise they contribute. So, there is a tradeoff between gain and noise reduction. With the current value of 6.8 megohms, as long as the lead resistance, $R_L$, can be kept down to a few megohms, the gain will be sufficient to obtain good measurements. The next largest noise contributer is the lead resistance, which generates about half as much noise as the gate current drive resistances. Finally, the amplifier current noise is two orders of magnitude smaller than the lead resistance noise.

## 3.8. Effects of Probe Parameters on Probe-Amplifier System

A sensitivity analysis can be done on equation 2-9. Sensitivity is defined as the change in one variable per unit change in another variable. In equation form, the sensitivity of z with repect to x is:

$$S_x^z = \frac{\frac{dz}{z}}{\frac{dx}{x}} = \frac{dz}{dx}\frac{x}{z} \qquad (3-21)$$

The sensitivity function does not give absolute magnitude information. Rather, sensitivity information can be used to tell how a function will vary with respect to many variables, one at a time. In the case of equation 2-9,

the sensitivity of $V_o$ with respect to every variable in the equation is what is needed. By using equation 3-21, these sensitivities are:

$$S_E^{V_o} = 2$$

$$S_h^{V_o} = 2$$

$$S_\alpha^{V_o} = 1$$

$$S_\theta^{V_o} = -2\theta\tan\theta \simeq -2.59$$

$$S_{C_{ant}}^{V_o} = \frac{2C_j}{C_{ant}+C_j} = 1.78$$

$$S_{C_j}^{V_o} = \frac{-2C_j}{C_{ant}+C_j} \simeq -1.78$$

$$S_{R_a}^{V_o} = \frac{2R_1+R_L+R_v}{2R_a+2R_1+R_L+R_v} = 0.40$$

$$S_{R_x}^{V_o} = \frac{-40k}{R_x+40k} \simeq -0.998$$

$$S_{R_1}^{V_o} = \frac{-2R_1}{2R_a+2R_1+R_v+R_L} = -0.035$$

$$S_{R_L}^{V_o} = \frac{-R_L}{2R_a+2R_1+R_v+R_L} = -0.352$$

$$S_{R_v}^{V_o} = \frac{-R_v}{2R_a+2R_1+R_v+R_L} = -0.014$$

Some of the sensitivities are equal to a constant, such as the first three. Some of the sensitivities are equal to an equation with variables, such as the last eight. This means that those values obtained for the sensitivities are only good for an incremental region around the variables in the equation. For example, $S_{C_{ant}}^{V_o}$ will change if either $C_{ant}$ or $C_j$ changes. However, the sensitivity will not change very much unless some of the variables change by a great deal. As can be seen by the sensitivity analysis, the magnitude

of the output voltage, $V_o$, will be most affected by changes in the angle $\theta$. This makes it very important to mount the dipole onto the lead structure correctly. The next most sensitive parameters are the E-field and the dipole length, h. The output voltage is almost six times more sensitive to change in dipole length than it is to lead resistance changes. The next most sensitive parameters are $C_j$ and $C_{ant}$. Notice that if $C_{ant}$ increases, the output voltage increases, but if $C_j$ increases, the output voltage decreases, as can be determined by the sign of the sensitivity function.

The most likely parameter to change on the probe is the lead resistance, $R_L$. Should $R_L$ become too large, not enough signal will reach the inputs to the amplifier, as can be seen by equation 2-9. This parameter can be controlled by controlling the overall length of the leads, along with the resistance per square. Should the leads not be equal in total resistance, then there will be an imbalance in the input lead structure. This will manifest itself in offset voltage, which can be nulled out. A value for this offset voltage, due to lead imbalance, at the input to the amplifier is:

$$V_{os} = \frac{6.8\delta R}{\left[6.8+\dfrac{R_L}{2}+\delta R\right]\left[6.8+\dfrac{R_L}{2}\right]} \tag{3-22}$$

This equation was derived assuming that one side of the lead resistance was equal to $\dfrac{R_L}{2}$ and the other side was equal to $\dfrac{R_L}{2} + \delta R$. All resistance values are in megohms. This value of offset voltage should be multiplied by 500 if an oscilloscope is connected to the output of stage 1 and this offset is measured.

The effect of changes of other probe parameters on the system can be calculated by changing these values in the appropriate equations. No major problems will result from minor variations in parameters. Should something major be changed, such as Gimpelson's mask used to fabricate leads, or perhaps a new type of diode, the effects can be theoretically predicted from the equations already derived, along with the sensitivity relationships presented in this section.

## 3.9. External Noise

Most external noise problems in the probe-amplifier system have arisen because of electrostatic energy storage. From basic electrostatic principles, charge on a conductor (assuming positive charge) produces lines of flux that start on the conductor and terminate on a more negatively charged surface, such as ground or another conductor. These lines of flux are an E-field. An E-field will produce a voltage. A system of charged conductors produce mutual voltages on each other, depending on their geometries and distances from each other. Induced charges can be produced in grounded conductors. If one of the voltages in the system changes, induced charges can change. If an induced charge changes, a current (time rate of change of charge) will flow in the ground plane [13]. Therefore, change of voltage produces change in induced charge and change in charge produces mutual voltage changes. The ratio of charge to voltage is capacitance. A mutual capacitance exists between all charged conductors, whether they are part of the intended circuit or not. Therefore, change of induced charge can possibly affect a circuit,

especially at the input where the signal is the weakest. This is a key concept. Mutual capacitances effectively couple every conductor within a certain distance into the intended circuit. This is not obvious and needs to be carefully watched and controlled. Charged conductors will produce a voltage on the input leads of an unshielded amplifier. These are the most critical signal lines affected, since any voltage potentials produced will be amplified and cause problems at the output. Electrostatic shielding is critical.

A problem that occured when the amplification system was being built and tested on a breadboard was the power distribution network in the laboratory radiated a 60 Hz signal that the unshielded amplifier picked up and amplified. The problem was extremely severe until an electrostatic shield, in conjunction with a filter, was used. Morrison [13] develops three rules for shielding and grounding of instrumentation systems (or any system). The third rule is not applicable to the probe-amplifier system, since it deals with ac power supplies, and the amplifier system uses 9 volt batteries for power.

The first rule states that an electrostatic shield enclosure should be connected to the zero-signal reference potential of any circuitry contained within the shield [13]. This is not necessarily earth ground, but the zero-signal reference potential. To see why this is so, consider figure 3-7. This is a pictorial representation of an amplifier surrounded by an electrostatic shield. The mutual capacitances between the three signal conductors and the shield are shown. The mutual capacitances among the conductors are not shown, to avoid cluttering up the diagram. There is feedback coupled
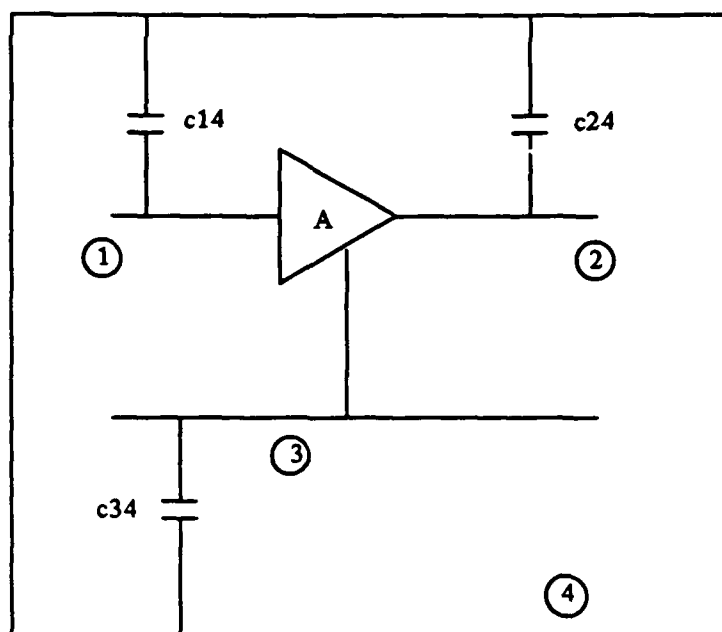
Figure 3.7    Amplifier Within an Electrostatic Shield

through the shield, as can be seen by tracing a path from conductor 2 through the shield, which is conductor 4, back to conductor 1. This is better shown in figure 3-8. This feedback is eliminated by connecting conductor three (zero signal reference potential) to conductor four (the shield). This is depicted in figure 3-9.

Rule 2 states that the shield conductor should be connected to the zero signal reference potential at the signal-earth connection [13]. A pictorial representation of what happens if this rule is not followed is shown in figure 3-10. Notice that Rule 1 was followed, because the shield is connected to the zero signal reference potential. However, if there is a
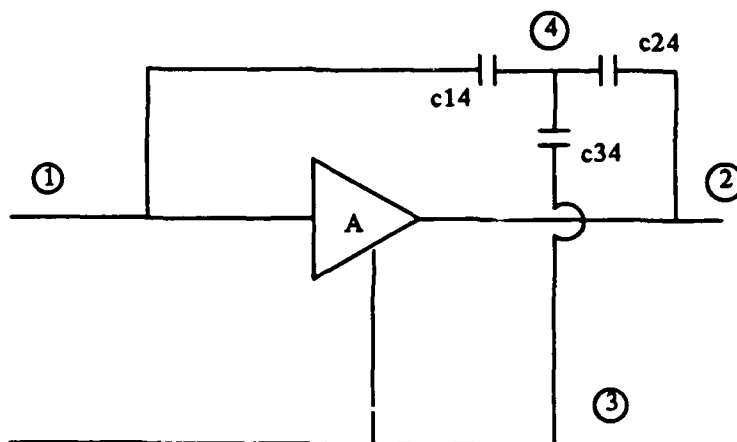
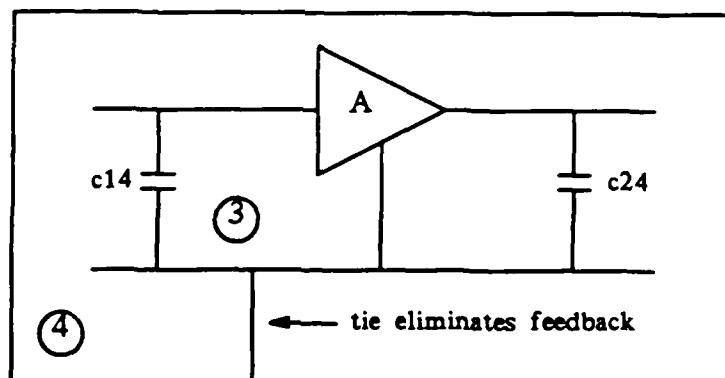Figure 3.8   Mutual Capacitances as Circuit Elements

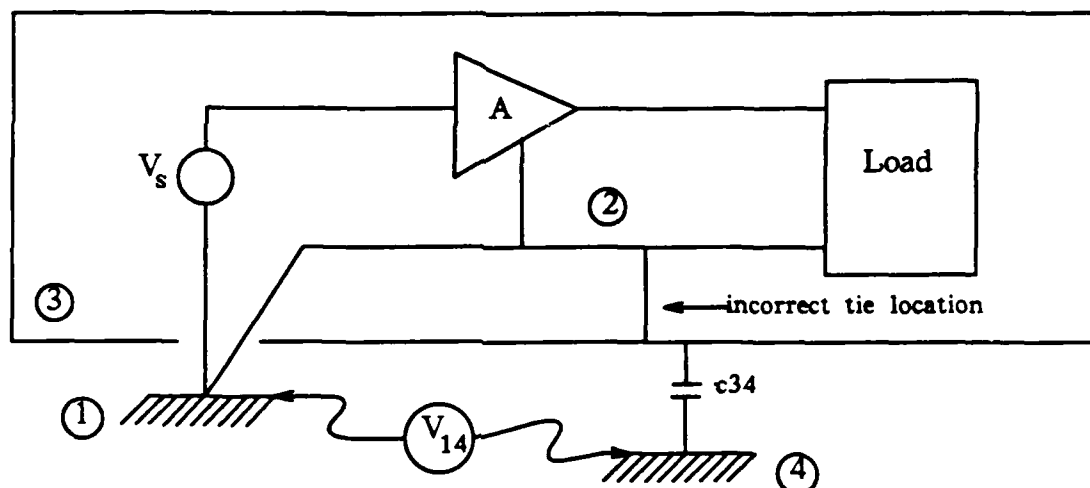Figure 3.9   Elimination of Undesirable Feedback

**Figure 3.10**   Incorrect Tie Between Shield and Zero Signal Reference Potential

potential difference between the two ground points, a current can be induced into the zero signal reference conductor. This current will combine with the signal current, and may cause problems in the circuit.

Unfortunately, in the probe-amplifier system, it is impossible to follow either of these rules, because the source is the junction region of the Schottky barrier diode, which is a floating source. So, the oscilloscope ground (ground referenced to the load, instead of the source) was used as the reference potential. As long as the probe is totally insulated from the shield, this will work. This requires using a rubber grommet around the copper input connector to which the probe is attached to keep the probe connector insulated from the shield. There is still a possibility of current flow through the mutual capacitance between the probe connector and the

shield, but experimental observation has proven that this is not a problem using any of the lab setups to take probe E-field measurements.

### 3.10. Three Axis Probe Requirements

The differences in the requirements for a three axis probe amplification system are really not that great. A three axis probe needs at least a six pin connector on the input stage of any amplification system. Once the signal lines are inside of the electrostatic shield they can be split apart. It would be most convenient to be able to have the amplification system split up into three independent channels, one for each axis of the probe. This will allow independent control of the gain and offset of each channel separately. Depending on the orientation of the probe in the E-field, this will allow maximum flexibility of measurements. The printed circuit board layout will have to be controlled very carefully. Not only do the input signal lines and power lines have to be carefully laid out to avoid mutual interference, but the separate channel input signal lines have to be laid out in such a way that the three channels do not interfere with each other. The recommendation of the author is to place each channel on its own pc board. It may be necessary to provide independent power supplies, depending on the power consumption of the internal circuitry of the system. The probe-amplifier system now can run on a set of 9 volt batteries all day. A three axis system should be able to run two to three hours before the batteries are run down to below 6 volts, which is the minimum acceptable voltage. Additionally, it would probably be best to obtain any output measurements

on each channel separately, and then mathematically manipulate them by hand using vector calculus if necessary. Other than these guidelines, a three axis amplification system seems to be a straightforward extension of the work already done.

The next chapter provides experimental results for the probe-amplifier system.

# CHAPTER 4

## EXPERIMENTAL RESULTS

### 4.1. Construction of the Amplifier

After deciding on the circuit configuration, a pc board was laid out.
Special attention was paid to the power and signal lines relative to each
other. The only major problem was experienced while soldering the
components to the board. In order not to obtain cold solder joints, a liberal
amount of flux was used on the conductors. This flux was not cleaned off
properly. Because of the extremely high input impedances involved, the
fluxed board provided a low impedance path relative to the unfluxed portion
of the board. The signal took the path of least resistance and the
amplification system saturated to one of the power supply voltages. After
checking a considerable number of other causes, the true culprit was
determined. A thorough cleaning with ethanol resolved this problem. It
should be noted that there was not that much flux around the conductors.
This problem must be closely watched on pc boards with high impedance
components separated by small physical distances. These distances are
necessarily small, since the whole idea behind submillimeter E-field
measurements with a probe-amplifier system is to be able to have a small,
portable system that can be easily placed into an area to obtain
measurements.

## 4.2. Variation of Gain with Power Supply Voltage

While attempting to calibrate one of the E-field probes produced in the laboratory, it was noticed that one of the measurements taken on a previous day seemed to not be repeatable. After examination of the probe-amplifier system, it became apparent that the voltage gain changed significantly with power supply voltage. An experiment was set up to record this change. The maximum power supply voltage is 9 volts. The minimum power supply voltage is 6 volts. Measurements of gain variation were taken by putting a signal into the system and using 9 volts as a benchmark voltage. The gain with 9 volts was taken to be the standard gain. The power supply voltage was varied in one volt increments down to 6 volts and the gain was measured. These values were normalized by dividing by the benchmark voltage. The results are plotted in figure 4-1. As can be seen from the plot, the gain changes by approximately 30% over the range of supply voltages. This is significant in that proper calibration of the probes needs to take this into account. Before any calibration work is done, a power supply voltage measurement needs to be taken. If, on a later date, more calibration needs to be done on a particular probe, another power supply voltage measurement needs to be taken, and the appropriate number, from figure 4-1, needs to be factored into the gain equation.

## 4.3. Noise Measurements

Noise measurements on the probe-amplifier system were taken using an HP 3580A Spectrum Analyzer. A baseline noise measurement on the
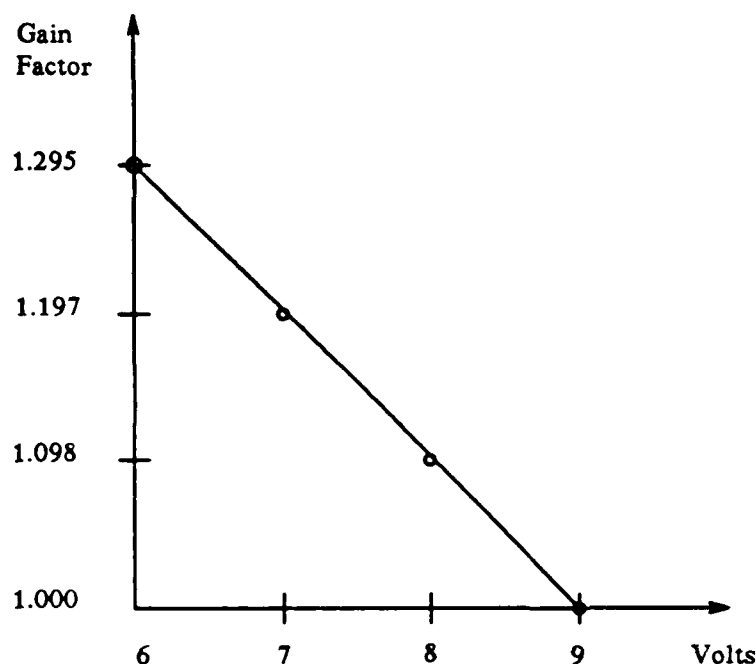
Figure 4.1   Plot of Normalized Gain vs Power Supply Voltage

analyzer was first taken. The analyzer generates its own internal noise from the circuitry inside. The lower limit on the analyzer's ability to measure noise is its own internal thermal noise. This is a theoretical limit. Other sources of noise will definitely be internally generated or externally impinge upon the analyzer, depending upon the environment in which it is operating. Figure 4-2 is a photograph of the analyzer with the power on and nothing connected to the input. The left side of the graticule is at 0 Hz. Each major vertical line on the graticule represents 10 Hz. A total spectrum of 100 Hz is shown. Notice the internally generated $\frac{1}{f}$ noise and the 60 Hz
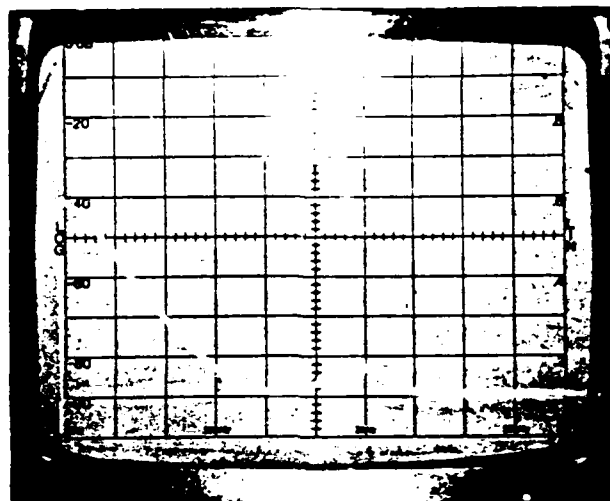
**Figure 4.2**  Baseline Noise Spectrum of HP 3580A Spectrum Analyzer

pickup. The input sensitivity is normalized to 0 dBV, so that the noise is actually directly readable from the left side (LOG side) of the graticule. The gain setting is adjusted to read dBV, where dBV is defined as 20 log $\frac{V_2}{V_1}$ and $V_1$ is 1 volt. Figure 4-3 is a picture of the probe-amplifier system connected up to the spectrum analyzer. In order to calculate the probe-amplifier system noise, the baseline must be subtracted from figure 4-3. Since the bandwidth of the system is 0.49 Hz, the noise only needs to be integrated from 0 Hz to 0.49 Hz. This part of the curve can be approximated by a straight line with minor error. The baseline value is approximately -40 dBV and the system value is approximately -39 dBV. Converting these values to rms voltages, the baseline is 10.0 mV and the
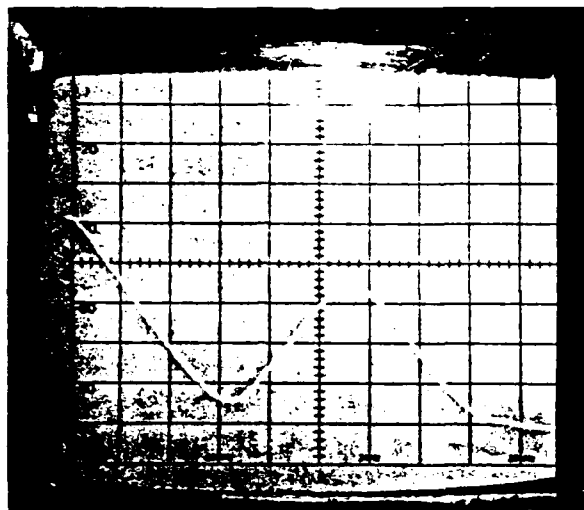
**Figure 4.3** Probe-Amplifier System Noise Spectrum

system value is 11.2 mV. Taking the difference and squaring it, the output

voltage power spectral density, $\frac{\overline{v_{on}^2}}{\Delta f}$, is $1.4 \times 10^{-6}$ $\frac{V^2}{Hz}$. Multiplying this value

by $\Delta f$, and then dividing this value by the system gain squared, as equation

3-13 states, a value for $\overline{v_{iin}^2}$ is found. Since $\overline{i_{iin}^2}$ is $\frac{\overline{v_{iin}^2}}{R_v^2}$, $\overline{i_{iin}^2}$ is $7.9 \times 10^{-23}$ $A^2$.

This makes the rms value of the noise current referred to the input, $i_{tin}$,

equal to 8.9 picoamps.

Equating the signal value from chapter 1 to the measured noise value,

as in chapter 3, the minimum E-field can be calculated:

$$\frac{\alpha}{4R_v} E^2 h^2 \left| \frac{C_{ant}}{C_{ant}+C_j} \right|^2 = 8.9 \times 10^{-12} \qquad (4-1)$$

Solving for the minimum E-field, a value of 16.2 volts/meter is found. This measured value is about 6 times larger than the theoretical minimum E-field value of 2.8 volts/meter that was calculated in the last chapter. Considering the random nature of the signals that are being discussed, in addition to the number of approximations that were made in order to make the problem tractable, the correlation of the theory to the measurements is not bad, in the opinion of the author. One of the major sources of error is the spectrum analyzer. An error in the baseline or the system value of 1 dBV will change the measured noise value by about 10%. This is significant when trying to interpolate a waveform's true value on the graticule. Another major source of error is the external noise in the laboratory that was present when these measurements were taken. This noise is picked up by the probe lead structure, which is not shielded. There is no way to measure this external noise. The only way to eliminate it is to go to a facility that has a anechoic chamber, such as the Bureau of Radiological Health. However, this defeats the purpose of having a small, portable system that can be easily transported and operated.

## 4.4. Verification of Gain Equation

In order to verify the gain equation, an experiment was set up in a waveguide, for which the E-field is well known. The concept of the experiment is to calculate the E-field by using two separate methods and compare the results. The first method involves measuring the power in the waveguide and calculating the E-field using the theory of waveguides. The

second method involves inserting the probe into the waveguide, measuring the output voltage of the probe-amplifier system and then use equation 2-9, the gain equation, to calculate the E-field in the waveguide.

A slotted waveguide system was assembled, with waveguide dimensions a = 2.25 cm and b = 1 cm. Figure 4-4 is a diagram showing the setup. A klystron was activated at 11.27 GHz, which corresponds to a wavelength, $\lambda$, of 26.6 mm. Power measurements were taken at different power levels. Also, at each power level, voltage measurements of the probe-amplifier system were taken.

Using waveguide theory, the equation for the E-field in the waveguide is:

$$E^2 = \frac{2P_o}{ab}\frac{\lambda_g}{\lambda}Z_o \qquad (4\text{-}2)$$

where $\frac{P_o}{ab}$ is the power density and $\frac{\lambda_g}{\lambda}Z_o$ is the impedance in the waveguide. $\frac{\lambda_g}{\lambda}$ is:

$$\frac{\lambda_g}{\lambda} = \frac{1}{\left[1-\left|\frac{\lambda}{2a}\right|^2\right]^{1/2}} \qquad (4\text{-}3)$$

and $Z_o$ is the impedance of free space, 377 ohms. The actual power in the waveguide is 23 dBm greater than the meter reading indicates, because there is a 20dBm attenuator attached between the waveguide and the meter, along with a 3dBm loss in the waveguide itself. So, in order to obtain the value
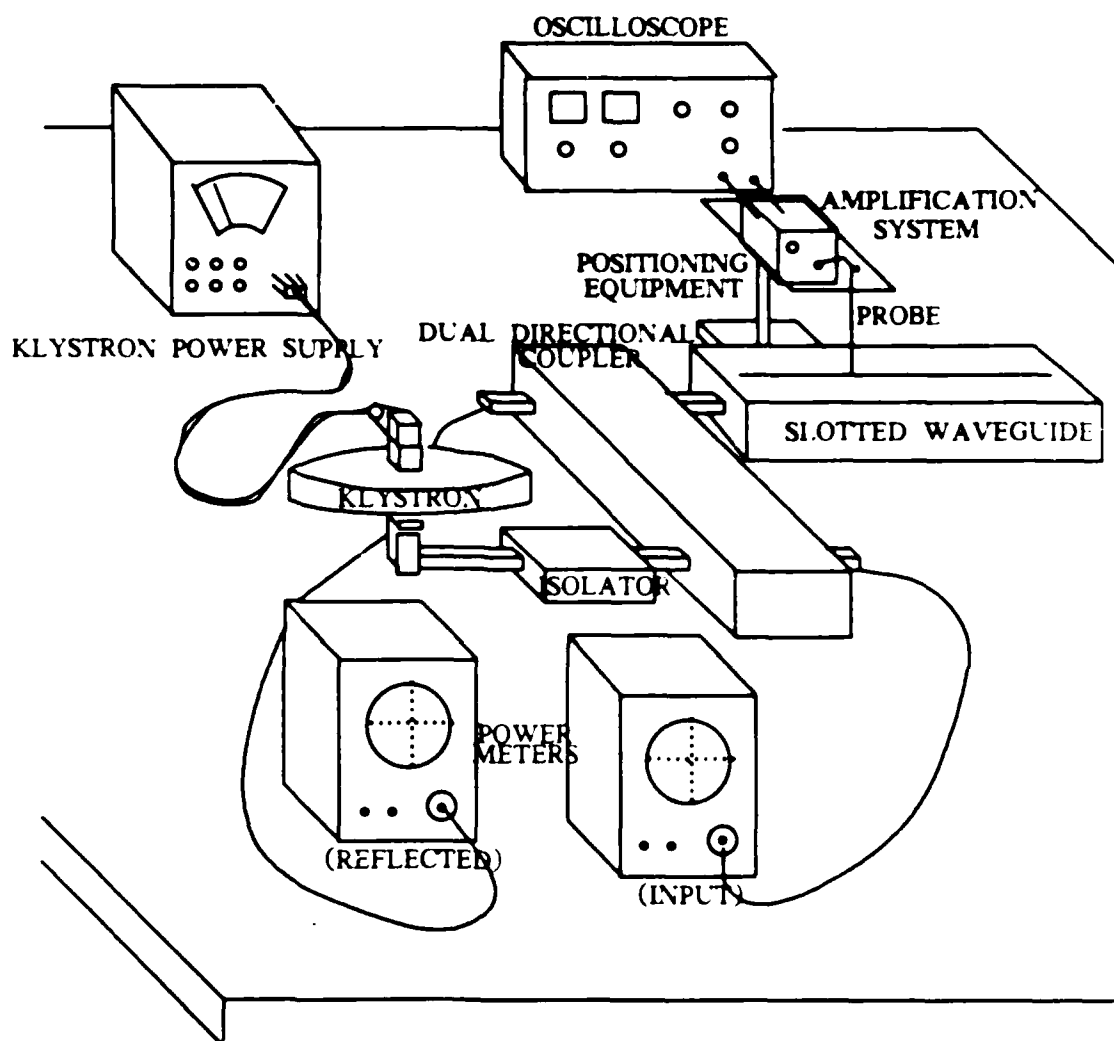
**Figure 4.4** Setup Used to Verify Gain Equation

of $P_o$, 23 must be added to the dBm reading on the meter. The voltage

measured on the oscilloscope, along with the power measured are as follows:

| Power (dBm) | Millivolts |
|---|---|
| -23 | 7.8 |
| -20 | 12.5 |
| -15 | 46.0 |
| -10 | 130.0 |

As mentioned above, these power and voltage readings are measured data, not calculated from any formulas. Using equations 4-2 and 4-3, and adding 23 dBm to the readings, as explained above, the power readings are converted to equivalent E-field strengths. The results are shown in the table below, on the left.

Also, using equation 2-9, along with the fact that a factor of 1.098 needs to be used due to the battery power supply voltage being at approximately 8 volts, in addition to dividing the output voltage by the factor cosine 54 degrees, due to the orientation of the dipole on the lead structure, the voltage measurements were converted to equivalent E-field strengths. The results are:

| (meas.) Power (dBm) | (calc.) E-field (V/m) | (meas.) Millivolts | (calc.) E-field (V/m) |
|---|---|---|---|
| -23 | 64 | 7.8 | 67 |
| -20 | 91 | 12.5 | 85 |
| -15 | 162 | 46.0 | 164 |
| -10 | 288 | 130.0 | 275 |

As can be seen from these results, the calculated E-fields using the results of the work in this thesis come very close to the E-fields calculated by using the waveguide formula.

## 4.5. Calculation cf Minimum E-Field Using Time Domain Parameters

In the noise measurement section, a spectrum analyzer was used to determine the noise in the system. From this value, assuming a SNR of one, the minimum detectable E-field was calculated. This is a frequency domain

approach to determining the minimum detectable E-field. In the last section, the gain equation was verified by an independant means of determining the E-field in the waveguide. The smallest voltage measurement taken was 7.8 millivolts, which corresponded to an E-field of about 67 volts/meter.

Using the same setup as in section 4-4, except substituting a meter, which is capable of reading down in the microvolt region, for the oscilloscope, the minimum detectable E-field should be able to be determined. After connecting the microvolt meter into the setup, and placing the meter into operation, a random fluctuation of approximately 0.3 millivolts was observed on the meter. This is the noise limit. Therefore, it is impossible to directly read a signal any lower than this value. Nulling out the offset of the amplifier as best as possible, the meter randomly fluctuated back and forth, around the zero point, due to the noise, as stated above. Then, increasing the power into the waveguide until the meter was fluctuating about the 0.3 millivolt point (rather than the zero point), this corresponds to the signal value roughly equalling the noise value. This also corresponds to the minimum E-field that can be directly measured, without using some other special instrument, such as a lock-in amplifier, to extract the signal from the noise. The results are:

| (meas.) Power (dBm) | (calc.) E-field (V/m) | (meas.) Millivolts | (calc.) E-field (V/m) |
|---|---|---|---|
| -37.2 | 12.6 | 0.3 | 13.2 |

As can be seen, a minimum detectable E-field of about 13 V/m was obtained using a time domain approach. This is very close to the approximately 16

V/m that was obtained using the frequency domain approach.

As is evident by the results of this chapter, the probe-amplifier system theoretical calculations are close to actual laboratory measurements. The noise calculations were verified using the spectrum analyzer and the gain equation was verified using the waveguide. The minimum detectable E-field was calculated using both a frequency domain analysis and a time domain analysis. The next chapter will explore possible ways to modulate the probe-amplifier system.

# CHAPTER 5

## MODULATION OF THE PROBE-AMPLIFIER SYSTEM

### 5.1. Introduction

In all the discussion so far, an ac E-field in the GHz region produced a dc signal in the nonlinear diode, which propagated down the transmission line and then was amplified. This chapter will explore the possibility of modulating the ac microwave E-field with a low frequency ac signal. There are theoretical calculations that can be experimentally verified by doing this, as will become apparent shortly.

### 5.2. Theory on Lock-In Amplifier

A lock-in amplifier allows measurement of signals imbedded in noise. It does this by means of an extremely narrow band detector which has the center of its passband locked to the frequency of the signal being measured. Because of the frequency lock and narrow bandwidth, large improvements in the SNR can usually be achieved. The lock-in amplifier used in this thesis is the Model 128A Lock-In Amplifier, manufactured by EG&G Princeton Applied Research.

An experiment was set up to test the validity of the concept of using a lock-in amplifier (LiA). A sine-wave generator was used as the modulating signal. This signal was fed to the klystron and was used to modulate the

72

11.27 GHz microwave frequency in the waveguide. This signal was also fed to the reference input of the LIA. In simplest terms, the LIA has a phase-locked loop internal to the device which produces a dc output that is proportional to the magnitude of the product of the reference signal and the unknown signal and the cosine of the phase angle of the reference signal minus the unknown signal. The composite signal (modulated and modulating) propagates down the waveguide and impinges upon the E-field probe. The probe picks up the modulating signal and also produces the usual dc signal, $V_{jo}$. These signals propagate down the lead structure toward the amplifier. The three-pole amplifier filter is bypassed in order to be able to amplify the modulating signal. The amplified signal is then fed into the unknown signal port of the LIA. The LIA strips off the dc signal and the unknown signal (detected and amplified modulating signal) is compared to the reference signal in the detector module of the LIA. If these signals are in phase, as described above, a dc output voltage is produced at the output of the LIA.

This setup has the capability to produce some interesting information concerning the probe. By varying the modulating signal frequency, the bandwidth of the probe lead structure can be determined. Smith [5] calculated this as $\frac{1}{4\pi R_L C}$, as mentioned in chapter 3, and Gimpelson [2] used this formula to calculate the probe bandwidth, which was equal to approximately 35 Hz. This can be verified in the lab using the setup above, as stated. Also, the phase shift between the reference signal and the unknown signal can be measured in the lab using the LIA setup. Since the modulating signal has to be kept below about 35 Hz, in order not to be

attenuated by the lead structure, and the filter on the amplifier is bypassed, the amplifier contributes essentially no phase shift to the system at these low frequencies. Therefore, any phase shift between the reference signal and the amplified signal, which is fed into the unknown signal port of the LIA, is due almost entirely to phase shift in the probe itself or the klystron. This phase shift can be measured and plotted against frequency.

## 5.3. Verification of Lead Structure Bandwidth

Using a setup as described above, the bandwidth of the lead structure was measured. A voltage reading was taken at low frequency (approx. 5 Hz). Then the frequency was increased until the voltage reading was at $\frac{1}{\sqrt{2}}$ of the low frequency voltage reading. The result was that the bandwidth of the lead structure is approximately 20 Hz. This basically verifies Smith's formula and *Gimpelson's* work.

## 5.4. Determination of Phase Shift

As is discussed above, the approximate phase shift between the reference and unknown signals can be determined. However, after setting up to measure phase vs frequency, it became apparent that this was going to be a long and tedious process. This is because of the time constants associated with the LIA. So, instead, a single frequency, 35 Hz, was chosen to use to measure the phase shift. The result was that the phase shift from the reference to the unknown signal ports was approximately 101 degrees. How much of this is probe phase shift and how much is klystron phase shift was

not able to be determined. This opens up an entirely new area of probe characterization that could be explored.

Using the setup described above, the relative phase shift between any two points in a cavity in which there is a modulated E-field should be able to be determined, as long as the modulating E-field is larger than the minimum detectable modulating E-field. A study to determine the minimum detectable modulating E-field (not to be confused with the minimum detectable modulated E-field, which was determined in this thesis) also could be done.

Modulating the probe has been shown, through laboratory testing, to be feasible. This opens up many areas that could possibly be explored. This chapter just touched on some of them.

# CHAPTER 6

## CONCLUSION

### 6.1. Summary

The purpose of this thesis was to design and analyze amplification and signal conditioning equipment that can be used with the current generation of E-field probes. The system was designed, built and tested. A complete noise analysis of the system was accomplished. In addition, modulation of the E-field probe was shown to be feasible, and was demonstrated in the laboratory.

An analysis of the requirements that the probe placed upon any amplification equipment was first done. The probe model was verified and a suitable amplifier design was developed on paper. This design was breadboarded and problems overcome by redesign. The amplifier was then built on a pc board and suitably housed and shielded in an appropriate container (metal box). A theoretical gain equation was developed relating the output voltage of the system to the impinging E-field on the probe.

The probe-amplifier system was then tested in various cavities, such as a waveguide and a slow-wave structure, using various frequency E-fields in the microwave region. The system was transported to Boston and tested at the Varian Corporation's Microwave Division, where it performed well.

Noise in the system was modeled and a complete noise analysis was done. A theoretical equation for the total equivalent mean square noise referred to the input was developed.

The noise equation was verified in the laboratory, in addition to the gain equation. The minimum detectable E-field was calculated and verified using both a time domain and frequency domain approach. Both approaches yielded essentially the same results.

Finally, modulation of the probe-amplifier system was shown to be feasible in the laboratory using a lock-in amplifier. This enabled some previous theoretical work to be verified. This also allows relative phase shift between two points in a cavity to be determined. This is significant in that not only the magnitude, but also the phase of an impinging E-field could possibly be calculated, once the phase contributions of the measuring equipment and klystron are determined.

## 6.2. Future Work

The work documented by this thesis can be logically extended into the realm of modulation of the probe-amplifier system. A complete phase analysis may yield some very interesting results. Measuring the amplitude and phase of E-fields inside of cavities with complex geometries may be able to greatly simplify certain problems, since the mathematical equations for these geometries may be difficult or impossible to find a closed form solution for. Additionally, measuring E-fields inside of biological media is another area that needs to be fully explored. Other applications and areas of

research concerning submillimeter E-field probe-amplifier systems can surely be found.

# REFERENCES

[1] H. Bassen and others, "Evaluation of an Implantable Electric-Field Probe within Finite Simulated Tissues", *Radio Science Supplement*, November-December 1977. pp. 15-26.

[2] G. Gimpelson, *The Design, Fabrication and Testing of a Submillimeter Implantable Electric Field Probe*, Doctoral Dissertation, School of Engineering and Applied Science, University of Virginia, 1983.

[3] P. Howerton, *Integrated Optical Electric-Field Strength Probe*, Doctoral Dissertation, School of Engineering and Applied Science, University of Virginia, 1986.

[4] T. H. Marshburn, *A Noise Analysis of an Electromagnetic Field Strength Probe of Submillimeter Dimensions*, Master's Thesis, school of Engineering and Applied Science, University of Virginia, 1984.

[5] G. S. Smith, "Limitations on the Size of Miniature Electric-Field Probes", Submitted paper, February 1984.

[6] Burr-Brown Integrated Circuits Data Book, Burr-Brown Corporation, Tucson, Az., 1986.

[7] A. Budak, *Passive and Active Network Analysis and Synthesis*, Houghton-Mifflin, 1974, pp. 254-8.

[8] P. R. Gray & R. G. Meyer, *Analysis and Design of Analog Integrated Circuits*, 2nd. Ed., Wiley, 1984.

[9] S. Soclof, *Applications of Analog Integrated Circuits*, Prentice-Hall, 1985.

[10] C. D. Motchenbacher & F. C. Fitchen, *Low-Noise Electronic Design*, Wiley, 1973.

[11]   W. R. Bennett, *Electrical Noise*, McGraw-Hill, 1960.

[12]   M. J. Buckingham, *Noise in Electronic Devices and Systems*, Ellis Horwood Limited, 1983.

[13]   R. Morrison, *Grounding and Shielding Techniques in Instrumentation*, 3rd Ed., Wiley, 1986.